FMH606 Master's Thesis 2020

Energy and Environmental Technology

Modelling and Evaluation of Compressed Air Energy Storage System

Marianne Fjellestad Heitmann

Faculty of Technology, Natural Sciences and Maritime Sciences
Campus Porsgrunn

Course: FMH606 Master's Thesis, 2020

Title: Modelling and evaluating of Compressed Air Energy Storage System

Number of pages: 62 (45 + Appendices)

Keywords: Compressed Air Energy Storage, CAES, Energy Storage, Dynamic Model

Student:	Marianne Fjellestad Heitmann
Supervisor:	Carlos F. Pfeiffer and Elisabet Syverud
External partner:	-
Availability:	Open

Summary:

With the worldwide increase on the use of renewable energy, efficient energy storage is needed to include intermittent renewable energy sources, such as wind and solar energy. One of the energy storage technologies that could solve this is the use of Compressed Air Energy Storage (CAES) systems. An Adiabatic Compressed Air Energy Storage (A-CAES) system has been analyzed in this report. The air is stored in a cavern of constant volume, and the heat produced by the compression of air in the charge process is stored in a packed bed and used to reheat the air for energy production in the discharge part.

This report presents a preliminary thermodynamic analysis estimating the size of the system for a given quantity of energy storage, a dynamic model including the packed bed for energy storage, and a simulation made in MATLAB to analyze the efficiency of the system. The traditional CAES has a roundtrip efficiency between 40-54%, while for the A-CAES analyzed in this report, the roundtrip efficiency is 53.4%. The physical limitations of the equipment (operation temperature and pressure of the required compressors and turbo expanders) were taken into account in this model. A preliminary cost estimation of the system was conducted, and the cost estimation was 2 699 NOK/kWh.

Preface

This master thesis was written in the spring 2020 as the final project to attain a MSc. in Energy and Environmental Technology at the University of South-Eastern Norway (USN).

The software used for calculations and simulations in this thesis is mainly MATLAB.

I would like to thank my supervisors Carlos F. Pfeiffer and Elisabet Syverud. I am so grateful for all their help and inputs during this project. It was really motivating to have supervisors with such knowledge and interests on the subject.

Porsgrunn, 15.05.2020

Marianne Fjellestad Heitmann

Content

Nomenclature

A-CAES	Adiabatic Compressed Air Energy Storage
Atm	Atmospheric pressure, 101.325 kPa
CAES	Compressed Air Energy Storage
D-CAES	Diabatic Compressed Air Energy Storage
GW	Gigawatt
kWh	Kilowatt hour
MW	Megawatt
TES	Thermal Energy Storage

1 Introduction

The increase in renewable energy sources, can result in a number of problems, mainly because of the variability of these sources. [1] To include the intermittent renewable energy sources, such as wind and solar energy, efficient energy storage systems are needed.

Use of batteries are one method to store the energy, but so far it is not practical to store large amount of energy to cover the seasonal variation in power consumption and production. [2] Another method to store surplus energy from intermittent sources are Pumped-storage Hydropower (PSH). Where the excess energy is used to pump water to high level reservoirs and can later be used to produce electricity using turbines. [3] Flywheel Energy Storage (FES) is another technique for storing the excess energy. The excess energy is used to accelerate large mass rotating cylinders, and later using the kinetic energy to move generators and produce electricity. [4]

The Compressed Air Energy Storage (CAES) systems, uses the excess electric energy to compress air in large deposits, and when electricity is needed, the air goes through a turbine, producing electric energy. [5] This is a very promising technology for energy storage, especially at large scale. [6]

The main purpose of this master thesis is to investigate proposed techniques for Compressed Air Energy Storage Systems (CAES) and how to integrate it to the electrical grid. This is the main tasks:

- Complete a literature review of different approaches for CAES systems
- Select some of the most promising CAES technologies, and develop a dynamic model for simulation
- Simulate the behaviour of the CAES systems with different scenarios, such as storage size and storage time.
- Provide a preliminary economic feasibility analysis for the selected CAES systems.
- Propose strategies to integrate CAES systems to an electric distribution grids, including system response time

The complete task description is in Appendix A.

Chapter 2 contains an overview of the different energy storage systems, and an introduction to some of the technologies of Compressed Air Energy Storage systems

Chapter 3 gives an insight on the electrical grid in Norway and some of the challenges that may occur in wind energy production

Chapter 4 presents an overview of the system for this project

Chapter 5 contains the dynamic model for the system

Chapter 6 gives an explanation of the simulations of the dynamic model

Chapter 7 contains the cost estimation for the system

Chapter 8 presents the result from the calculations, simulations and the cost estimation

Chapter 9 contains a discussion of the results

Chapter 10 contains the conclusion

2 Energy Storage

This chapter contains an overview of different energy storage, and some of the technologies of Compressed Air Energy Storage (CAES) Systems, such as the Diabatic Compressed Air Energy Storage (D-CAES) system, Adiabatic Compressed Air Energy Storage (A-CAES) System, and Isothermal Compressed Air Energy Storage (I-CAES) system. Storage options are also mentioned.

2.1 Battery Energy Storage

Batteries can be used to store the intermitted energy sources, and when its needed, the energy is released again. All four of the technologies, lithium, lead, nickel and sodium, has the ability to provide important functions for grid operators, and have potential for further economic and technological developments. Lead based batteries have been used in industrial applications for more than hundreds of years and is well established in grid applications for grid operators and end-user. Because of the low cost, this battery is used for almost all the small-scale PV installations that needs batteries. For largescale renewable energy storage installations, the use of either sodium or lithium-ion batteries are more commonly because of their lower specific energy and power, usually lower cycle life and longer charging time. Nickel-based batteries are used in special situations where energy is stored in extreme climate, fast-charging conditions or long-cycle. [7] Batteries are most suited to store energy for a couple of hours and for a storage capacity of 5kWh -10 MWh. [2]

Due to the increase in renewable energy sources, the global energy storage market is growing. In 2018, the global battery capacity was 1 905.5 MW and according to the forecast, this number will increase over the next years. [8]

2.2 Pumped-Storage Hydropower

The basic principle of the Pumped-Storage Hydropower (PSH) is simple. When the energy demand is low, the surplus energy is used to pump water from a lower level reservoir to a higher level reservoir. When the energy demand is high, the water is released back to the lower level reservoir, producing electricity using turbines. There are some losses in this process, but turbines and generators are quite efficient so the efficiency of these plants will usually be 70-80%. [3] PSH are ideal to store energy for days to months, and with a storage capacity at 50 MWh – 10GWh. [2]

According to the International Hydropower Association (IHA), the global installed PSH capacity in 2018 was 160.3 GW, up 1.9 GW from 2017. China, Japan and The United States are the main contributors, with 30.0, 27.6 and 22.9 GW, respectively. [9] By 2030 this number is expected to increase by 78 GW. [10]

The main disadvantage of PSH is the specific nature needed, there must be both height and water availability. Suitable places for these plants are likely to be in mountains with scenic surroundings. With this follows social and ecological issues. [11]

2.3 Flywheel Energy Storage

In Flywheel Energy Storage (FES) a rotor accelerate at a very high speed and the energy is maintained in the system as rotational energy. When energy is added to the system, the speed

increases, and when energy is extracted, the speed is reduced. There are two classes of FES: low-speed flywheels, and high-speed flywheels. [4] FES are mostly used to store energy for minutes and has a smaller energy capacity from approximately 1 – 100 kWh. [2]

2.4 Compressed Air Energy Storage

In a Compressed Air Energy Storage (CAES) System the excess electrical energy is used to compress air to a high pressure. Then the air is stored in caverns or tanks. When the energy is needed, the pressurized air is released, reheated and expanded in the turbines, which generates electric energy. This energy is then returned to the grid. This storage system has the storage capacity of 5MWh – 1GWh, and for a discharge time of hours and days. [2]

In the traditional Diabatic CAES (D-CAES) system there are two processes. The first one is the charging mode. Air is compressed by the compressor, driven by an electric motor, which uses the surplus energy. The compressed air is cooled and then stored in a cavern. When the electricity is needed, the compressed air goes through a heater to reheat the air. The heated air goes through a turbine, which generates electric energy. This is the second process which is call the discharge mode. This design needs fuel to reheat the air, which usually results in an efficiency around 40 percent. Figure 2.1 shows the general idea of a D-CAES system. [12] [5]
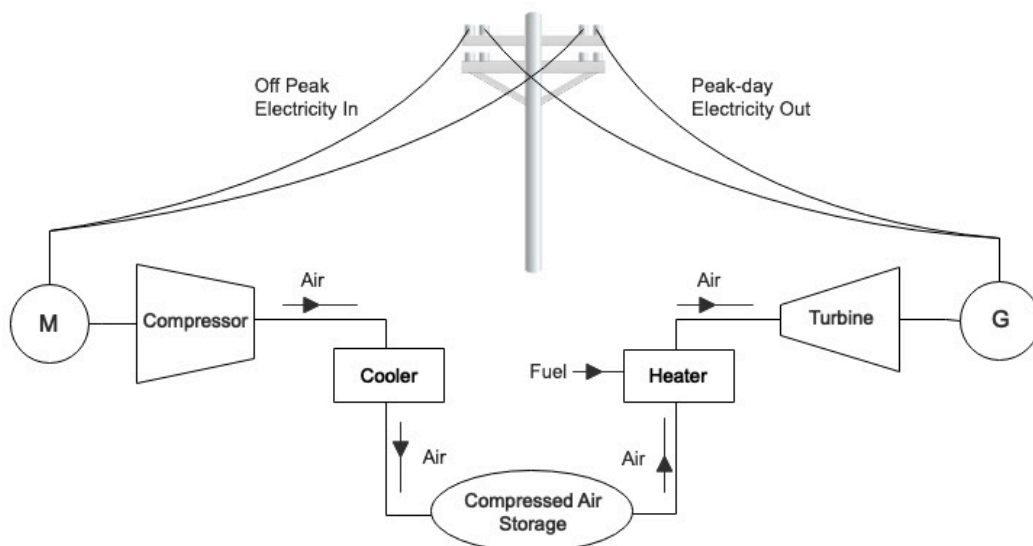
Figure 2.1: A general CAES system, where air is compressed, cooled down and stored in a cavern, and later reheated to produce electricity by the turbine.

All existing plants in the world today are made using existing equipment already in use for other applications. The Huntorf Plant in Germany was the first compressed air storage power station in the world, and the commercial operation started in December 1978. The output of the D-CAES plant is 290 MW. The air is stored in two salt caverns with a total volume of about 310 000 m^3. [5] The roundtrip efficiency of this plant is 42%. [13] The maximum inlet temperature for LP is 850°C, while for HP it is 550°C. The operation pressure is 4.8 – 6.6 MPa. [14]

The second D-CAES plant in the world is the 110 MW McIntosh plan in Alabama, US. This plant was completed in June 1991.The air is compressed in three stages and stored in a salt cavern with a total volume of about 530 000 m^3. At full power, this plant has a power generating

duration of 26 hours. The reheat expander train has high- and low-pressure expanders, with combustors, which can use both natural gas and oil as fuel, and drives the electric generator producing electricity. To extract thermal energy from the low-pressure expander, an advanced recuperator is used to preheat the inlet air form the caverns before it goes into the high-pressure combustor. This reduces the fuel consumption by about 22 – 25 %. [5] [15] The roundtrip efficiency of this plant is 54%. [13] The maximum temperature for LP is approx. 870°C, and around 540°C for HP. The operation pressure is 4.5 – 7.4 MPa. [14]

2.4.1 Adiabatic CAES

In an adiabatic process, there are no heat transfer between the system and its surroundings, meaning dQ = 0. [16]

In an Adiabatic Compressed Air Energy Storage (A-CAES), thermal energy storage (TES) is used to replace the combustor. During the compression, a lot of energy is expelled as heat. This heat is stored in TES and later used to reheat the air during expansion. This will contribute to both higher efficiency of the plant, and less environmental impact due to the fact that fuel is not needed. There has been a lot of research on this type system, but so far only to the stage of simulation of models and theoretical analysis. [17] ADELE is a German project where the goal is to build an A-CAES system with an efficiency around 70%. When the air is compressed, the heat is captured in a heat-storage facility instead of being released to the surrounding. Later during the discharge, the energy in the heat-storage is released into the compressed air. With this solution, no gas combustion is needed to heat the air. By avoiding the use of fossil fuel, this technology provides a CO_2 neutral delivery of the peak-load electricity from renewable energy [18]. The storage temperature of the plant is the most important parameter in an A-CAES. There are three main temperature categories, high temperature A-CAES operates above 400°C, medium temperature A-CAES runs between 200 – 400°C, while a low temperature A-CAES operates below 200°C [19]. In [20] an A-CAES with packed bed achieves an efficiency of 70%. It is simulated for a temperature range of 300 – 700 K. In [6] a low-temperature A-CAES is presented with a roundtrip efficiency of 52 – 60%. This operates at temperature from 90 – 200°C. In [21] it is found that the efficiency is in the range of 60 – 70% when the TES system has an efficiency over 90%. It operates at a temperature from 100 - 500°C.

2.4.2 Isothermal CAES

In an ideal isothermal CAES process the temperature is kept constant as the pressure increases in the compressor and decreases in the expansion. This requires cooling of the air in the compression process and heating of the gas in the expansion process. With an ideal isothermal CAES, the efficiency reaches 100%, and does not require a thermal energy storage, nor fossil fuel. One of the challenges is to transfer heat at a high rate with minimal temperature difference. To do this very large surface area of contact are required. [22] [23] [24]

2.4.3 Air Storage

As for the storage of pressurized air the most cost efficient is to use caverns already made, such as solution-mined salt caverns, which are used in the two existing CAES plants (Huntorf and McIntosh). This is one of the subsurface, constant volume storage methods. Other options are caverns made by excavation in hard rock, porous rock formation, depleted oil or gas fields, and abandoned mines. Another method is constant pressure storage, by water-filled tunnels with an above-ground pond or under-water balloons. The water level or volume will vary with the

charging status, and the pressure is kept constant. In smaller CAES plans, below 10MW and limited storage capacity (1-2h), the possibility of above-ground storage can be considered. The three pressure vessels options are air storage tanks, gas storage pipelines, and gas cylinders. [22] [25] [26]

3 Connection to the Grid

This chapter contain an overview of the grid in Norway as well as some of the challenges of wind energy and grid curtailment.

3.1 The grid in Norway

In Norway the power grid is regulated by the state, so the Norwegian water resources and energy directorate (NVE) grants licenses for production and transmission of renewable energy. The electricity grid in Norway consists of three levels: the transmission grid, the regional grid, and the distribution grid [27]. The transmission grid is what binds the major manufactures and consumer together in a system. This network also includes the international connections. This is a high voltage network, usually of 300 to 420 kV, but some in some parts lines of 132 kV are included. The regional grid is what connects the transmission network and the distribution network and may include production consumption at higher voltage level. This grid has a voltage of 33 kV to 132 kV. The distribution grid is the local power grid which usually provide power to small end user. This network has a voltage up to 22 kV. [28] The electrical energy supply in Norway is three-phase alternating current (AC), with a frequency of 50 Hz. [29]

In Norway, all grid systems, for every voltage level, need a licence, and everyone that owns or operates a network or produces or sell power needs a license for this. [30]

3.2 Wind Energy

Wind energy is an energy source that can vary greatly, which means that an ordinary generator will produce unregulated frequencies and voltages. This can be a problem for the stability of the system if it produces large amounts of energy, as for example in a wind park. With frequency regulation, the frequency can vary between 47.5 – 52.0 Hz without any outcome. [31]

The output of windfarms is sometimes curtailed. Grid curtailment is when the energy delivery from a generator to the grid is reduced or restricted. There are many reasons for why this could happen, but the one that is most interesting for this project is when the curtailment happens because of overload, e.g. when the supply is greater than the demand. [32] This will result in direct losses in the production of energy.

In these periods a CAES would come in handy. Instead of restricting the energy production and waste the energy, it can be used to power compressors. Then this energy would be stored as thermal energy in the TES until it is needed. In addition to store energy that potentially would be wasted, these systems can be used to stabilize the grid.

4 System Overview

This chapter contain an overview of the A-CAES system. The first part is the overall system with an explanation of how it operates. Then follows a closer look at each of the components in the system.

4.1 Overall System

In this A-CAES the surplus energy from wind turbines will power three compressors, which will compress the air from atmospheric pressure (1.01325 bar) to 70 bar. After each compressor there are a packed bed with Raschig rings in ceramics, that will cool down the air, and store the heat from the compression. The hot air out of the compressor enters at the top of the packed bed and exits at the bottom. The cooled air then enters the next compressor, is compressed and enters the next packed bed. This happens in three stages before the compressed air is stored in the cavern. This is the so-called charge process.

The discharge process is similar. When the air is released from the cavern it re-enters the packed beds, now to reheat the air. In this process the air enters at the bottom with a lower temperature and exits at the top with a higher temperature due to release of the stored heat from the charge process. The heated air is expanded in a turbine, which drives a generator that generates electric energy. The air is cooled down in the turbine, so the air enters the next packed bed to be re-heated. As in the charge process, this happens in three stages. The electric energy generated by the turbines are released back to the grid. This is shown in Figure 4.1.
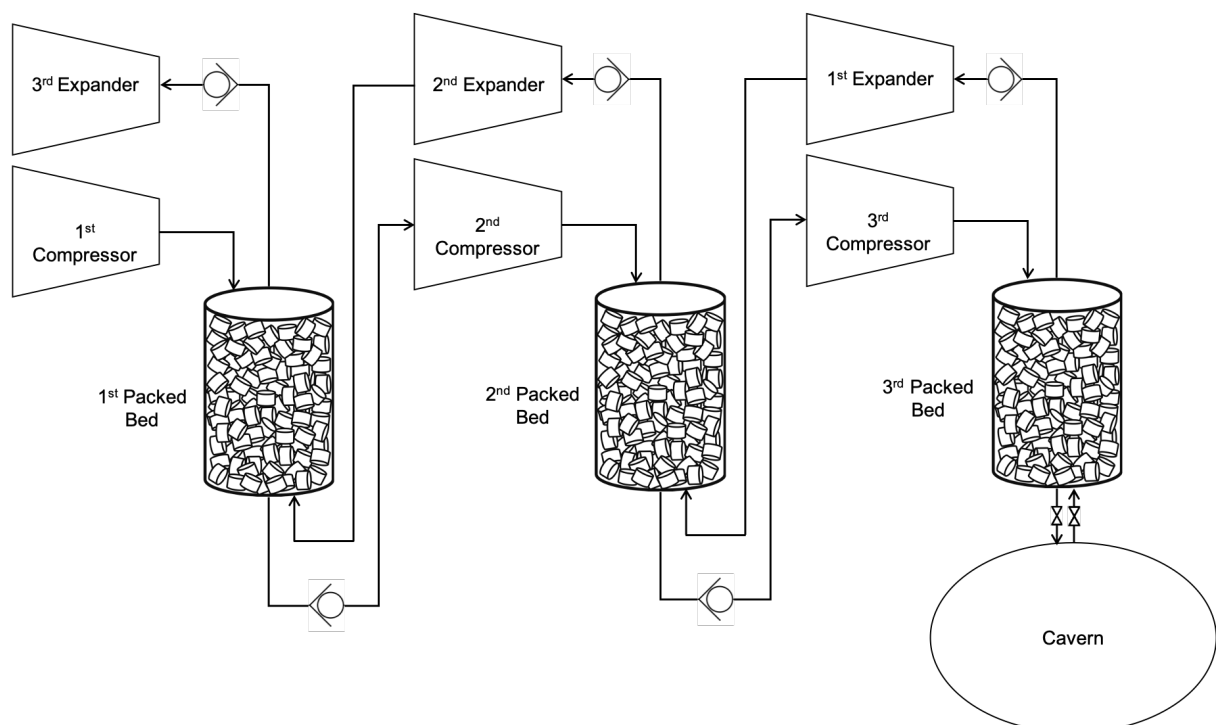
Figure 4.1: The A-CAES system with three compressors, three packed beds, a cavern and three expanders.

The minimum operational pressure in the cavern is 40 bar, while the maximum pressure is 70 bar. When the pressure is below 70 bar, and there is surplus electric energy, the charge mode

is activated. When the pressure in the cavern reaches 70 bar it stops. When the energy is needed, the discharge mode will begin. This will go on until there is surplus energy available, or the pressure in the cavern decreases to 40 bar.

Valves are used to control the flow of air. The check valve makes sure the flow of air only goes in one direction, while the control valves by the cavern open and closes the flow for charge and discharge mode. The Control valve by the first expander keeps the pressure into the expander constant at 40 bar. For the air to flow to the cavern, each increment of air must be compressed to a pressure just above the storage pressure. Therefore, there is a valve before the cavern to control that the pressure into the cavern is always higher than the pressure inside the cavern.

4.2 Compression

Based on the flow rate and the pressure ratio, multistage centrifugal compressors are suited for this system. [33] The centrifugal compressor achieves a pressure rise when the fluid, in this case air, passes through a rotating impeller, which adds high velocity to the air. By slowing down the air in the diffuser, an increase in static pressure will occur. [34]

If the compression, from 1atm to 70 bar, were to happen in one stage without intercooling the temperature would rise to approximately 965 K. The compressor has a maximum operational temperature of 550K, so the compression must happen in multiple stages with intercooling.

The compressors performance is usually expressed in a characteristic curve. This typically display the range of speeds, flows, efficiencies and heads. An example of a characteristic curve is shown in Figure 4.2 [35]. The head, discharge pressure, or the pressure ratio are usually on the y-axis, while the inlet flow is on the x-axis. The circles are the efficiency curves and the curved lines are the speed curves. The surge limit describes the flow at which the operation of the compressor becomes unstable. This happens when the flow of the compressor is not enough to produce a sufficient head. The stonewall, or choke, happens when the speed of sound is reached at the exit of the compressor wheel. If this happens, the flow cannot be increased even if the suction pressure is increased. This can cause a drop in efficiency and pressure ratio. [36]
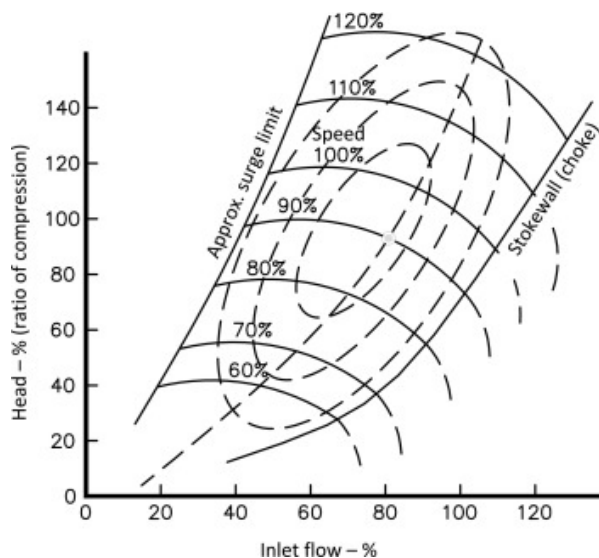
Figure 4.2 An example of a characteristic curve for a compressor. [35]

In this system the operating point is not fixed, it operates at a wide range of flows. Therefore, an average efficiency of 80% is used.

4.3 Heat Storage

The temperature of the air increases in the compression stages, and in order to avoid very high temperatures, intercooling and aftercooling between each compression is necessary. There are two methods to do this in an A-CAES: the indirect-contact exchangers, and direct-contact exchanger. The most common one is the indirect-contact exchangers, where walls separates the fluid from the gas and the heat transfer occurs through these walls. While in the direct-contact exchanger, the heat transfer happens when the gas is in direct contact with a fluid or a solid in a packed bed. [20]

Packed beds are columns packed with either solid particular matter or porous solid. The space between the particles are called voidage, void fraction or porosity. They are usually used in the chemical and food industries, i.e. desorption, adsorption, and rectification. As they offer very high rates of heat transfer, and good tolerances for temperatures and pressures, packed beds could be a good solution for a A-CAES. In addition, it would replace the need for both indirect-contact heat exchangers and a separate thermal storage. [20] [37]

In this case the column is packed with Raschig Rings, which are small, cylinder shaped rings. The rings are usually made of ceramic or metals, in this case Alumina has been used which offers high thermal conductivity and heat capacity, and low cost. They are random packed in the column which provides a large contact area between the gas and the solid, and results in a low pressure drop. [38] [39] [40] Figure 4.2 a) shows the random packing structure of the column and b) is a picture of ceramic Raschig rings.
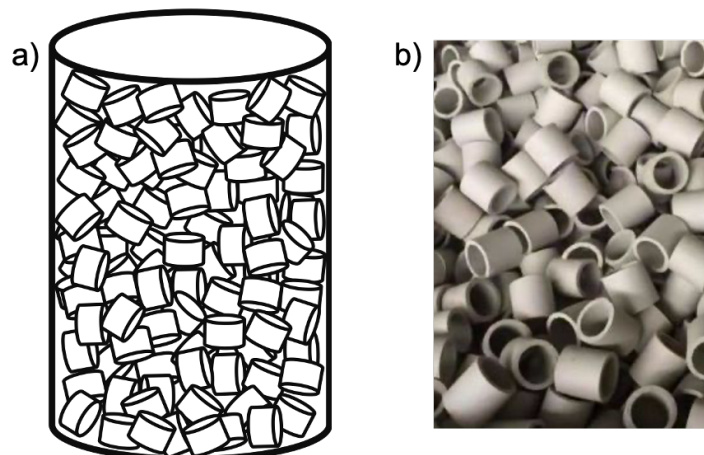
Figure 4.3: a) The random packing of the bed, b) example photo of ceramic Raschig Rings from a suppler [41].

4.4 Compressed Air Storage

In this project it is decided to use a constant volume cavern as storage for the compressed air. There is a lot of mountains in Norway, so the potential of hard rock caverns is huge. There are also some abounded mines and tunnels which can be used. By using an existing mine or tunnel the cost of the system will be reduced. There are no salt caverns onshore in Norway, therefore, hard rock cavern is used in this project. [26]

4.5 Expansion

For expansion there are two main equipment design in use today; industrial steam turbines and turbo expanders developed for industrial power turbines. The typically inlet pressure for an industrial steam turbine is from 40 – 60 bar and the inlet temperature is 500°C. The pressure ratio for a turbo expander is 6:1, and the inlet temperature is from 450 – 550°C. [42] The inlet temperatures of these expanders are higher than the temperature stored in the packed beds, due to the limitations on the compressor. In a D-CAES the temperature is increased to this temperature by burning fuel, but this is not desired in an A-CAES. The performance of the expander is highly affected by the operational properties of the air. It is therefore important to follow systematic guidelines when choosing an expansion machine. Because of the temperatures these turbines would most likely run off-design in this system and have a lower efficiency. [14]

Turbo expanders are designed for constant corrected flow function $(m\sqrt{T}/p)$. The constant flow rate is shown in Figure 4.4, and it also shows that the turbine maintains the efficiency (η_t) for a wide range of the pressure ratio. [34]
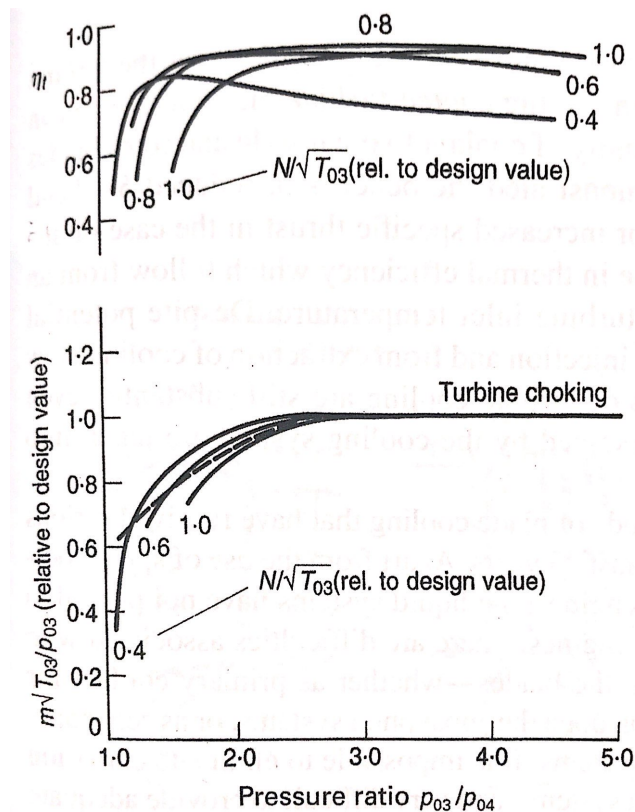
Figure 4.4: Turbine characteristics. [34]

There is a turbo-expander where each stage is of radial mixed flow design. The LP has typical inlet pressure of 75 bar, mass flow of 27.4 kg/s and output of 8.34 MW. This is of interest for this system. [43]

Based on this information an efficiency of 80% is assumed for the expansion in this system.

5 Dynamic Model

This chapter contains the dynamic model of the CAES System. The first part contains the equations for sizing the cavern, and the dynamic model for the mass and temperature inside the cavern. The next part is for the compression, then the model for the packed beds, and then the last part is for the expansion.

5.1 Cavern

5.1.1 Sizing the Cavern

To decide the size of the cavern to store the compressed air for two days (48 hours), the ideal work produced by the turbines in the discharge process were calculated. In these calculations a perfect, reversible process is assumed.

The energy balance for the discharge process are given by:

$$\frac{dE}{dt} = -\dot{n}\left(\Delta\widehat{H} + \Delta\widehat{E}_p + \Delta\widehat{E}_k\right) + \dot{Q} + \dot{W} \tag{5.1}$$

Where $\frac{dE}{dt}$ are the change in energy over time (kJ/s), $\dot{n}$ is the number of moles (kmol/s), $\Delta\widehat{H}$ is the change in enthalpy (kJ/kmol), $\Delta\widehat{E}_p$ and $\Delta\widehat{E}_k$ is the change in potential and kinetic energy (kJ/kmol), Q is the heat transfer (kW) and W is the work (kW). In this case the change in energy over time are assumed to be zero $\left(\frac{dE}{dt} = 0\right)$, as well as the change in potential and kinetic energy $\left(\Delta\widehat{E}_p = \Delta\widehat{E}_k = 0\right)$. The equation can be simplified to:

$$\dot{n}\,\Delta\widehat{H} = \dot{Q} + \dot{W} \tag{5.2}$$

The entropy balance for the discharge process is given by:

$$\frac{dS_{cv}}{dt} + \dot{n}\,\Delta\widehat{S}_{fs} + \frac{\sum Q_{i,surr}}{T_{\sigma,surr}} = \dot{S}_\sigma \tag{5.3}$$

Where $\frac{dS_{cv}}{dt}$ are the change in entropy over time for the control volume (kJ/kmol s K), $\Delta\widehat{S}_{fs}$ are the change of entropy in the flow(kJ/kmol K), $Q_{i,surr}$ is the heat transfer from the surroundings (kW), $T_{\sigma,surr}$ are the temperature of the surroundings (K), and $\dot{S}_\sigma$ is the total generation of entropy (kJ/kmol K). When assuming a perfect, reversible process, the change in entropy over time is assumed zero $\left(\frac{dS_{cv}}{dt} = 0\right)$, as well as the total generation of entropy ($\dot{S}_\sigma = 0$). Then the equation becomes:

$$\dot{n}\,\Delta\widehat{S}_{fs}T_{\sigma,surr} = -\sum Q_{i,surr} \tag{5.4}$$

By assuming $Q_{i,surr} = -Q_{sys}$ and $\dot{n} = 1$, eq. (5.4) becomes:

$$\Delta S_{fs} T_{\sigma,surr} = Q_{sys} \tag{5.5}$$

And by inserting eq. (5.5) into eq. (5.2), the ideal work (kW) can be calculated by:

$$W_{ideal} = \Delta \hat{H} - \Delta \hat{S}_{fs} T_{\sigma,surr} \tag{5.6}$$

Where the enthalpy and entropy are found by eq. (5.7) and (5.8):

$$\Delta \hat{H} = C_p (T_2 - T_1) \tag{5.7}$$

$$\Delta \hat{S}_{fs} = C_p \ln \frac{T_2}{T_1} - R \ln \frac{p_2}{p_1} \tag{5.8}$$

Where C_p is the specific heat capacity for constant pressure (kJ/kmol K).

When the ideal work has been calculated, the molar flow rate (mole/s) can be calculated by:

$$\dot{n} = \frac{W_{desired}}{W_{ideal}} \tag{5.9}$$

Where $W_{desired}$ are the desired work for this case, and W_{ideal} are the ideal work calculated by eq. (5.6).

To calculate the mass of the air, the following equation are used:

$$m = \dot{n}\, m_w t \tag{5.10}$$

Where m is the mass of air (kg), m_w is the molecular weight of air (kg/kmol) and t is the time (s).

To find the volume of the cavern, the ideal gas law is used:

$$V = \frac{nRT}{p} \tag{5.11}$$

Where V is the volume (m^3), n is the number of moles, R is the universal gas constant (8.314 kJ/kmol K), T is the temperature (K) and p is the pressure (kPa).

The cavern is assumed to be spherical and the radius (m) are calculated by:

$$r = \sqrt[3]{\frac{V}{\pi}\frac{3}{4}} \tag{5.12}$$

5.1.2 Mass of the Cavern

Since the volume is constant the mass in the cavern will vary due to the pressure increase and decrease over time. The mass balance for the cavern are:

$$\Delta M = \dot{m}_{in}\Delta t \tag{5.13}$$

Where $\Delta(M)$ is the change in total mass (kg), $\dot{m}_{in}$ is the mass flow of air into the cavern (kg/s) and Δt is the change in time (s). This leads to:

$$\frac{dM}{dt} = \dot{m}_{in} \tag{5.14}$$

5.1.3 Temperature of the Cavern

The temperature of the cavern will vary as well as the total mass and pressure. The energy balance for the cavern is:

$$\Delta\left(M\,\widehat{U}\right) = \dot{m}_{in}(t)\widehat{H}_{in}(t)\Delta t \tag{5.15}$$

Which becomes:

$$\frac{d\left(M\,\widehat{U}\right)}{dt} = \dot{m}_{in}\widehat{H}_{in}(t) \tag{5.16}$$

Where:

$$\frac{d\left(M\,\widehat{U}\right)}{dt} = M\frac{d\widehat{U}}{dt} + \widehat{U}\frac{dM}{dt} \tag{5.17}$$

and $\widehat{U}$ is the internal energy and $\widehat{H}_{in}$ is the enthalpy into the cavern. $\widehat{U}$ can be calculated by

$$\widehat{U} = \widehat{U}_0 + C_v(T - T_0) \tag{5.18}$$

Where C_v is the specific heat capacity for constant volume (kJ/kmol K), $\widehat{U}_0$ is reference internal energy (kJ/kmol) and T_0 is the reference temperature (K). The enthalpy can be calculated by

$$\widehat{H}_{in} = \widehat{H}_0 + C_p(T_{in} - T_o) \tag{5.19}$$

Where $\widehat{H}_0$ is the reference enthalpy (kJ/kmol).

When inserting eq. (5.16), (5.18) and (5.19) into eq. (5.16), eq. (5.16) becomes:

$$M\,C_v\frac{dT}{dt} + \left(\widehat{U}_o + C_v(T - T_0)\right)\dot{m}_{in} = \dot{m}_{in}(\widehat{H}_0 + C_p(T_{in} - T_0)) \tag{5.20}$$

Eq. (5.20) can be simplified to:

$$\frac{dT}{dt} = \frac{\dot{m}_{in}(C_p T_{in} - C_v T)}{M\,C_v} \tag{5.21}$$

5.2 Adiabatic Compression

To calculate the temperature after the compression, the energy balance for the compressor is used. Since the work is added to the system, the work is positive:

$$dU = dQ + dW \tag{5.22}$$

Where dU is the internal energy (W), dQ is the heat transfer (W) and dW is the work (W). As previously mention, in an adiabatic process the heat transfer is zero ($dQ = 0$), the internal energy and work can be calculated by the following equations:

$$dU = C_p dT \tag{5.23}$$

$$dW = -RT\frac{dp}{p} \tag{5.24}$$

By inserting eq. (5.23) and (5.24) in eq. (5.22), The equation becomes:

$$C_p dT = -RT\frac{dp}{p} \tag{5.25}$$

Which is then used to calculate the temperature of the air after the compression T_1 (K):

$$T_1 = T_{in}\left(\frac{p_2}{p_{in}}\right)^{\frac{R}{C_p}} \tag{5.26}$$

Where T_{in} is the temperature of the air into the compressor (K), p_2 is the pressure after compression (kPa), p_{in} is the pressure before the compression (kPa).

Since the pressure in the cavern varies, the mass flow of air does as well. Therefore, the output of the compressor will change as well. The work from the compressor is calculated by:

$$W_{charge} = \dot{m}\,C_p(T_1 - T_{in})\frac{1}{\eta_{poly}} \tag{5.27}$$

Where η_{poly} is the polytropic efficiency of the compressor. It can be assumed that the isentropic efficiency over one stage is constant. But due to multiple stages and increase of pressure ratio this will not be correct for all the compressors. Therefore the efficiency for the compressor are the polytropic efficiency, which is the isentropic efficiency of an elemental stage, so that it is constant throughout the entire process. [34]

5.3 Packed Bed

The conservation of energy is used to express the equations for the temperature of the air and the solid phase in the packed bed:

$$\Delta E = \dot{m}_{in}\Delta\widehat{H} - \dot{m}_{out}\Delta\widehat{H} - \hat{h}\,A\,(T_f - T_s) \qquad (5.28)$$

On the right-hand side, the first two terms are the net heat input due to the fluid flow and the last term is the heat transfer to the solid.

The packed bed is used to cool down the air so the temperature of the air will be higher at the top of the bed than the bottom. To make the calculations of the temperature distribution simpler, the bed is divided into n sections. When assuming constant mass flow $\dot{m}_{in} = \dot{m}_{out} = \dot{m}$, the energy rate for the fluid in a section is

$$\varepsilon A\rho_a C_{p,a}\frac{dT_a}{dt}\,\Delta z = -v_a\rho_a A C_{p,a}\frac{dT_a}{dZ}\Delta z - \hat{h}_{vol}A\Delta z(T_f - T_s) \qquad (5.29)$$

Where, ε are the void fraction of the air, A are the area (m^2), ρ are the density (kg/m^3), $\frac{dT_a}{dt}$ are the change of the temperature of the fluid over time, Δz is the height of the section (m), v are the velocity (m/s), $\frac{dT_a}{dz}$ are the change of temperature of the fluid over the length (K/m), $\hat{h}_{vol}$ is the volumetric heat transfer coefficient (kJ/m^3 s K), and T is the temperature (K). Subscript a stand for air and s for solid.

For the solid the energy rate is:

$$(1-\varepsilon)A\Delta z\rho_s C_{p,s}\frac{dT_s}{dt} = -\hat{h}A\Delta z(T_f - T_s) - \varepsilon\,A\frac{d}{dz}\left(\lambda_s\frac{dT_s}{dz}\right) \qquad (5.30)$$

Where the last term is the heat conduction through the solids in the packed bed. The contact between the solids are very small, so this term can be neglected. Eq. 5.30 becomes:

$$(1-\varepsilon)\rho_s C_{p,s}\frac{dT_s}{dt} = -\hat{h}(T_f - T_s) \qquad (5.31)$$

To calculate the volumetric heat transfer coefficient, $\hat{h}_{vol}$, between the Raschig Rings and the air, the empirical relationship suggested by Coutier and Farber [44] were used:

$$\hat{h}_{vol} = 700 \left(\frac{G}{d_p}\right)^{0.76} \tag{5.32}$$

Where G are the core mass velocity of the air (kg/m²s), and d_p are the average particle diameter (m).

5.4 Flow of Air

The flow of air is calculated by the equation for sub-critical flow (p_1 < 2x p_2) from Appendix B:

$$Q_G = 962\, C_{V,valve} \sqrt{\frac{p_1^2 - p_2^2}{SG\, T}} \tag{5.33}$$

Where Q_G is the gas flow in standard cubic feet per hour, $C_{V,valve}$ is the coefficient of flow, p_1 is the inlet pressure in psia, p_2 is the outlet pressure in psia, SG is the specific gravity of the air at 70°F and 14.7 psia, and T Is the absolute temperature in °R. None of these are SI units, so conversion equations are used as well to get the answer in the correct unit.

5.5 Adiabatic Expansion

To calculate the temperature of the air after expansion the energy balance for the expander is used. This is similar to the energy balance for the compressor in eq. (5.22), but since the work is being extracted from the system, the work is negative:

$$dU = dQ - dW \tag{5.34}$$

Due to the adiabatic process $dQ = 0$, while dU and dW are calculated by eq. (5.35) and eq. (5.36):

$$dU = C_p dT \tag{5.35}$$

$$dW = -RT \frac{dp}{p} \tag{5.36}$$

By inserting eq. (5.35) and eq. (5.36) in eq. (5.34), the equation becomes:

$$C_p \frac{dT}{T} = RT \frac{dp}{p} \tag{5.37}$$

And to calculate the temperature after det expander, the following equation are used:

$$T_2 = T_{in} \left(\frac{p_2}{p_{in}}\right)^{\frac{R}{C_p}} \tag{5.38}$$

The work generated by the expander can be calculated by:

$$W_{discharge} = \dot{m} \, C_p (T - T_{in}) \, \eta_{isen} \tag{5.39}$$

Where η_{isen} is the isentropic efficiency. Since the expanders are adiabatic, the ideal process is isentropic, and the efficiency are called isentropic efficiency. [34]

5.6 Efficiency of the System

The efficiency of the system is calculated by:

$$\eta = \frac{W_{discharge}}{W_{charge}} \tag{5.40}$$

Where $W_{discharge}$ is the work produced by the expanders (kW), and W_{charge} is the work done by the compressors (kW).

6 Simulation

To simulate the model MATLAB R2018a for academic was used.

First a script for the charge process was made. Different pressure ratio for the compressors were tested to find suitable output pressures of the compressors so that the output temperature does not exceed 550 K.

In a separate script a function for the packed beds were made. Each of the packed beds were divided into five sections to make the calculation of the temperature distribution over the beds easier. For each bed, there is five equations to calculate the temperature of the air in each section and five equations to calculate the temperature of the solids. Eq. (5.29) and (5.31), which are the equation for the temperature of the air and the solid respectively, were discretised for each section of the packed beds:

$$\frac{dT_{a,n}}{dt} = \frac{-v_{a,n}\,A\,\rho_{a,n}\,C_a\,\dfrac{\left(T_{a,n} - T_{a,n-1}\right)}{\Delta z}\,\Delta z - h_{vol} * A * \Delta z\,(T_{a,n} - T_{s,n})}{\varepsilon\,A\,\Delta z\,\rho_{a,n}\,C_a} \qquad (6.1)$$

$$\frac{dT_{s,n}}{dt} = \frac{-h_{vol}\,(T_{s,n} - T_{a,n})}{(1 - \varepsilon)\,\rho_s\,C_s} \qquad (6.2)$$

Where subscript n is for section n in the packed bed, and $n - 1$ is the temperature into the section. There are 15 equations of eq. (6.1) and 15 equations of eq. (6.2), one for each section of each bed. In addition to the temperature of the air and solids of the bed, the mass and temperature in the cavern is calculated in this script, as well as the work done by each compressor.

The mass flow through the valve are calculated in an if-loop: If the pressure inside the cavern is lower than the maximum pressure of 70 bar, the flow is calculated by eq. (5.33), if not, the mass flow is zero.

The density of the air is dependent on the temperature and the pressure of the air. Since both the temperature and the pressure drops over the packed bed, the density needs to be calculated for each section of the bed. This is done by the following equation:

$$\rho_{a,n} = \frac{p_n}{R\,T_{a,n}}\,m_w \qquad (6.3)$$

The velocity of the air is changing over the bed as well and this is calculated for each section by:

$$v_{a,n} = \frac{\dfrac{\dot{m}}{\rho_{a,n}}}{A\,\varepsilon} \qquad (6.4)$$

The solver used to calculate these ordinary differential equations (ODE) were the ode45 solver. This solver is based on an explicit Runge-Kutta equation, the Dormand-Prince pair. This is a single step solver, meaning that it only needs the solution at the previous time point. It integrates the differential equations from initial time to final time. tspan, which is the interval

of integration from initial time (t0) to final time (tf), and the initial values (y0) are specified as vectors and must have the same length. [45] In this case the time interval is from 0 to 172 800 sec so it is added a timestep of 1800, which means it is only printing the solution every 30 minutes instead of each second. This makes the code run faster, but still gives correct results. The code looks like this for the charge process:

```
TM_0 = [283 283 283 283 283 283 283 283 283 283 283 283 283 283 283 283 283
283 283 283 283 283 283 283 283 283 283 283 283 m_ini T_ini 0 0 0];
Tspan = [0:1800:172800]
[t,TM] = ode45(@packed_bed,tspan,TM_0);
```

Where TM are the name of the output, TM_0 are the initial values. For the temperatures of the air and solid, and the temperature of the cavern (T_ini), the initial temperatures are set to 283 K (10°C), m_ini are the initial mass of the cavern, calculated by the ideal gas law. The last three values are the initial values for the work done by the compressor, which is zero. The tspan is from time 0 to 172800s with a timestep of 1800. packed_bed is the name of the function.

A new function for the discharge process is made and this is pretty similar as for the charge process, the difference is that the air enters at the bottom of the packed bed instead of the top as in the charge process, and the packed bed is used to heat the air instead of cooling it, so eq. (5.29) and (5.31) are discretised to:

$$\frac{dT_{a15}}{dt} = \frac{-v_{a15}\,A\,\rho_{a15}C_a\,\dfrac{(T_{a15} - T_{Ca})}{\Delta z}\,\Delta z - h_{vol} * A * \Delta z\,(T_{a15} - T_{s15})}{\varepsilon\,A\,\Delta z\,\rho_{a15}\,C_a} \qquad (6.5)$$

$$\frac{dT_{s15}}{dt} = \frac{-h_{vol}\,(T_{s15} - T_{a15})}{(1 - \varepsilon)\,\rho_s\,C_s} \qquad (6.6)$$

The mass flow through the valve in the discharge process are calculated in an if-loop: If the pressure inside the cavern is higher than the minimum pressure of 40 bar, the flow is calculated by eq. (5.33), if not, the mass flow is zero.

For the discharge process, the initial values are the end values for the charge process (except for the work produced by the turbines) so the code looks like this:

```
TMD_0 = [TM(end,1:32) 0 0 0];
tspan = [0:1800:172800];
t2,TMD = ode45(@packed_bed_discharge,tspan,TMD_0);
```

TMD is the name of the output for this process, and the function is called packed_bed_discharge.

The complete MATLAB code is in Appendix D.

7 Cost Estimation

In order to check whether the A-CAES system is economic feasible, a cost estimation is needed. A perfect estimation is difficult to accomplish, but a simple estimation for the system based on data from other systems, size and material is shown in this chapter to give an idea of the magnitude of the cost.

7.1 The Compressors

To estimate the cost of the compressors, a SIMIENS tool called Datum calculator is used. This tool is for the Datum compressor type, which are commonly used in the oil and gas industry. The tool is limited and can only deliver initials estimates, but it is sufficient enough to give an approximate cost. The tool calculates a three-stage compressor with three impellers and intercooling. The CAPEX of one compressor are assumed to be 500 000 $. [46] To get the price of the compressor ($C_{compressor}$) in NOK the cost in USD is multiplied with the conversion from USD to NOK:

$$C_{compressor} = C_{comp,\$} \; Conversion_{\$ \, to \, NOK} \tag{7.1}$$

7.2 The Packed Beds

The cost estimation for the packed beds are based on the volume of the column and the mass of the solid.

The height and radius of each column are 30m and 5m, respectively. This leads to a volume of 2 355 m^3. The Columns are assumed to be inside the mountain, so the cost of mountain blasting needs to be taking into account. In Norway this cost is relatively expensive at about 200-300 NOK per cubic meter (NOK/m^3) [47]. The total cost of mountain blasting for each packed bed, C_{column} (NOK), is calculated by:

$$C_{column} = V_{volumn} \; C_{blasting} \tag{7.2}$$

Where V_{column} is the volume of the column (m^3), and $C_{blasting}$ is the cost of mountain blasting (NOK/m^3).

The solid inside the column are Raschig Rings in ceramic with a void fraction of 74%. The ceramic is Alumina (Al2O3), with a density of 3 900 kg/m^3. The cost of the ceramic is 1.90 $/kg (Appendix C). The total cost of the solid, $C_{solid,total}$ (NOK), for each packed bed is calculated by:

$$C_{solid,total} = V_{column} \; \rho_{solid} \; (1 - \varepsilon) \; C_{solid,\$} \; Conversion_{\$ \, to \, NOK} \tag{7.3}$$

Where ρ_{solid} is the density of the solid (kg/m^3), ε is the void fraction, $C_{solid,\$}$ is the cost of the solid ($/kg), and $Conversion_{\$ \, to \, NOK}$ is the conversion from USD to NOK (10.2 NOK/$).

7.3 The Cavern

The cost of the cavern is the mountain blasting, which is the same as for the Packed bed. Eq. (7.2) is used to calculate the cost of the cavern. The volume of the cavern is calculated to be 41 264 m^3. The cost of the mountain blasting is the same (200-300 NOK/m^3).

$$C_{cavern} = V_{cavern}\, C_{blasting} \tag{7.4}$$

7.4 The Expanders

According to [43] the cost of a Mixed Flow Expander is somewhat the same as for the compressor. So the cost for one expander are assumed to be 500 000 $. [46]

8 Results

This chapter contains the results of the simulation and the cost estimation.

8.1 Simulations

The first step was to decide the size of the system and the storage time of the system. The capacity of the system was decided to be 12 MW, which is equivalent to the energy produced from about five wind turbines. The storage time was set to 48 hours (two days). To calculate the size of the cavern, eq. (5.1 - 5.12) were used, and the volume of the cavern was calculated to be 41 264 m^3 with a radius of 21.4 m.

Assumptions and limitations:
- The pressure drop over each of the packed beds are assumed to be constant at 100 kPa.
- The temperature in the cavern are assumed to reach 323.15 K (50°C) when its fully loaded (70bar) and assumed constant at discharge.
- The maximum output temperature of the compressor is 550K (276.85°C).
- When the charge process starts, the initial pressure of the cavern is 40 bar (4 000 kPa) and the process stops when the pressure in the cavern reaches 70 bar (7 000kPa).
- The charge process starts at 70 bar and ends when the pressure is decreased to 40 bar.

Table 8.1 contain the parameters used in the simulations.

Table 8.1 Parameters used in the simulations.

Parameter	Definition	Value	Unit	Source
T_{in}	Temperature in	288.15	K	
$C_{p,a}$	Specific heat air, constant pressure	29.138	kJ/kmol K	
C_a	Specific heat air, constant pressure	1.006	kJ/kg K	[48]
$C_{v,a}$	Specific heat air, constant volume	20.826	kJ/kmol K	
C_a	Specific heat air, constant volume	0.717	kJ/kg K	[48]
C_s	Specific heat solid	0.955	kJ/kg K	[40]
ρ_s	Density of the solid	3 900	kg/m^3	Appendix C
ε	Void fraction of the solid	0.74	-	[49]
d_p	Average diameter of the particle (solid)	50	mm	[49]

The pressure of the charge process was decided with trial and error method. It was discovered that three compressors would be needed so that the maximum temperature of the compressors were not exceeded. The first one will compress the air from 1 atm (101.325 kPa) to 500 kPa, the second compressor will compress the air from 400 kPa to 2 000 kPa and the last one from 1 900 kPa to 7 200 kPa. Due to the pressure drop over the packed beds, which is set to 100 kPa, the pressure into the second and third compressor will be lower than the output from the compressors. Table 8.2 contains the pressure parameters for the simulation.

Table 8.2: Pressure parameters for the simulation

	Definition	**Value**	**Unit**
p_{in}	Pressure in	101.325	kPa
p_{C1}	Pressure after 1st compressor	500.0	kPa
p_{C2}	Pressure after 2nd compressor	2 000.0	kPa
p_{C3}	Pressure after 3rd compressor	7 200.0	kPa
p_V	Pressure after the valve	4 100.0	kPa
p_{E1}	Pressure after 1st expander	1 000.0	kPa
p_{E2}	Pressure after 2nd expander	600.0	kPa
p_{E3}	Pressure after 3rd expander	101.325	kPa

The size of the packed beds was decided with the trial and error method. It was discovered that with a height of 30 m and a radius of 5 m, that the temperature would be cooled down to an acceptable temperature for the compressor.

8.1.1 The Mass of the Cavern

The total mass in the cavern are shown in Figure 8.1. The red line (a) is the increase of mass in the cavern during the charge process. It starts at an initial mass of 2.03 $\times 10^6$ kg, which is calculated by the universal gas law. After about 30 hours (~108 000 s) the cavern reaches the maximum operational pressure of the cavern (70 bar) and the maximum mass of the cavern is also reached. When this value is reached the charge process stops.

The blue line (b) shows the decrease of mass in the cavern during the discharge process. It starts at the maximum mass of 3.09 $\times 10^6$ kg, and after about 47 hours (~169 000 s) the cavern reaches the minimum operational pressure of 40 bar. The x-axis shows the time in seconds from 0 to 172800 s (48 hours).
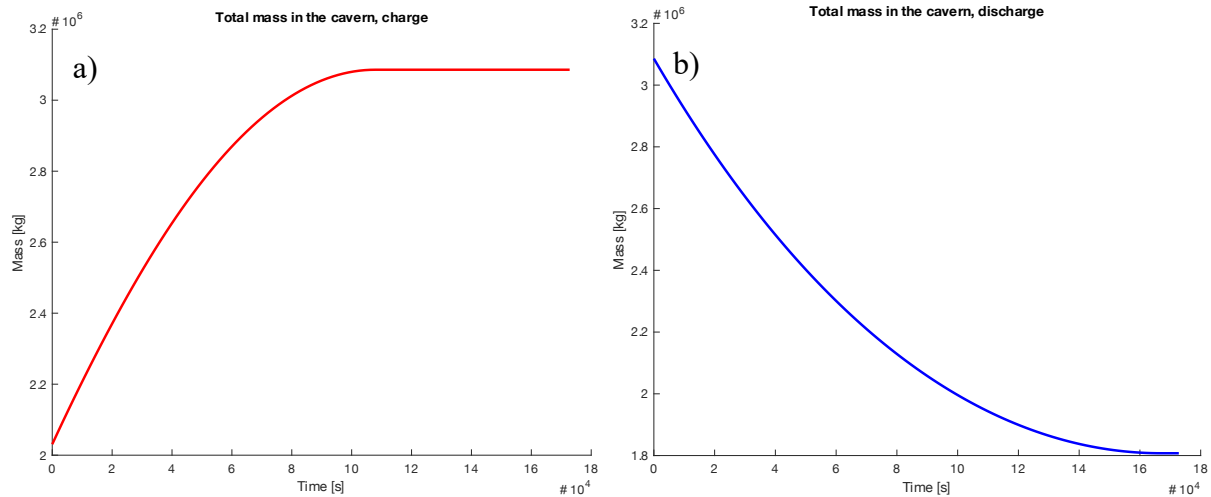
Figure 8.1: The total mass in the cavern, a) is for the charge process, b) is for the discharge process.

8.1.2 Temperatures in the Charge

The temperature out of the first compressor are calculated by eq. (5.26). With an inlet temperature of 288.15K, inlet pressure of 101.325 kPa and outlet pressure of 500 kPa this temperature is 454.5 K. This is the temperature that enters the first packed bed.

The temperature over the first bed is shown in Figure 8.2. The green line shows the temperature of the air in the first section of the packed bed. This is where the air enters at 454.5 K. The purple line shows the temperature of the air in the second section of the bed. This section will reach a temperature of 428.7 K. The red line shows the temperature of the air in the third section, and reaches a temperature of 390.1 K. The pink one shows the temperature of the air in the fourth section, which reaches a temperature of 350.3 K. The turquoise line shows the temperature of the air in the last section. This temperature ends at 319.6 K. This is the temperature of the air that enters the second compressor. The black dotted lines are the temperature of the solid in the corresponding section.

The initial temperature of the air and the solid are set to 283 K. The simulation is done for 48 hours. The charge process ends after about 30 hours because the cavern is fully loaded with air at 70 bar. This means that the flow of air stops, and the temperature of the air and the solid in the packed beds will stop increasing. The beds are assumed to be well insulated, so the temperatures stay constant. In the first packed bed, the first section reaches the temperature of the input of the packed bed, which is 454.5 K.
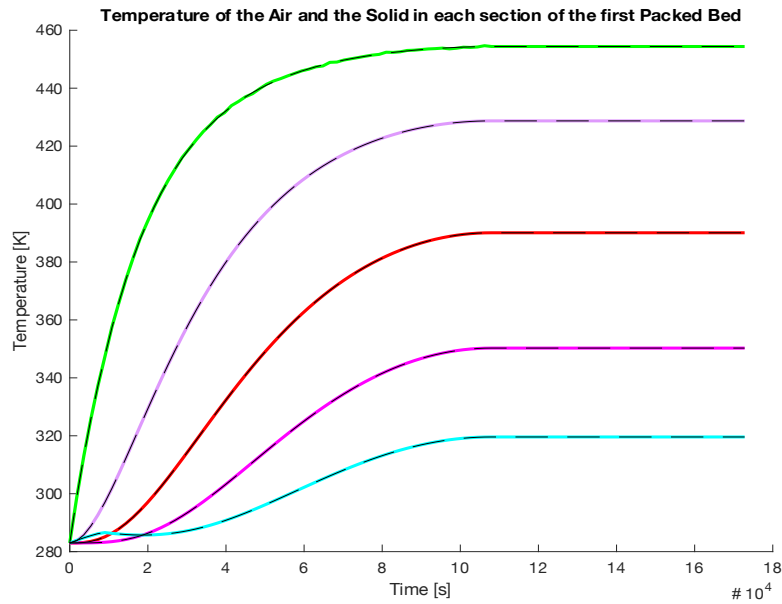
Figure 8.2: The temperatures of each section of the first packed bed in the charge process, where the green line is the first section, the purple is the second section, the red line is the third section, the pink is the fourth section and the turquoise line is the last section. The black dotted lines are the temperature of the solid to the corresponding section.

The temperature of the air that exits the first packed bed is the temperature of the air entering the second compressor. The temperature of the air out of the second compressor is calculated by eq. (5.26). This will vary due to the variation of the temperature into the compressor, but it will be in the range of 447 – 505 K.

The temperatures over the second packed bed are shown in Figure 8.3. As for Figure 8.2, the green line is the temperature of the air for first section of the packed bed. This section reaches a temperature of 468.6 K, which is lower than the maximum temperature that is entering. The purple one is the temperature of the air for the second section. This section reaches a temperature of 430. The red one is the temperature of the air for the third second, which reaches a temperature of 387.3 K. The pink one is the temperature of the air for the fourth section and reaches a temperature of 347.2 K. And the turquoise one is the temperature of the air in the last section of the packed bed. This temperature is 317.1 K when it exits the packed bed. This packed bed reaches higher temperatures due to a higher input temperature of the compressor. But since the cavern is filled after 30 hours and the mass flow of air stops, the second packed bed never reaches the temperature out the first compressor. The black dotted lines are the temperature of the solid to the corresponding section.
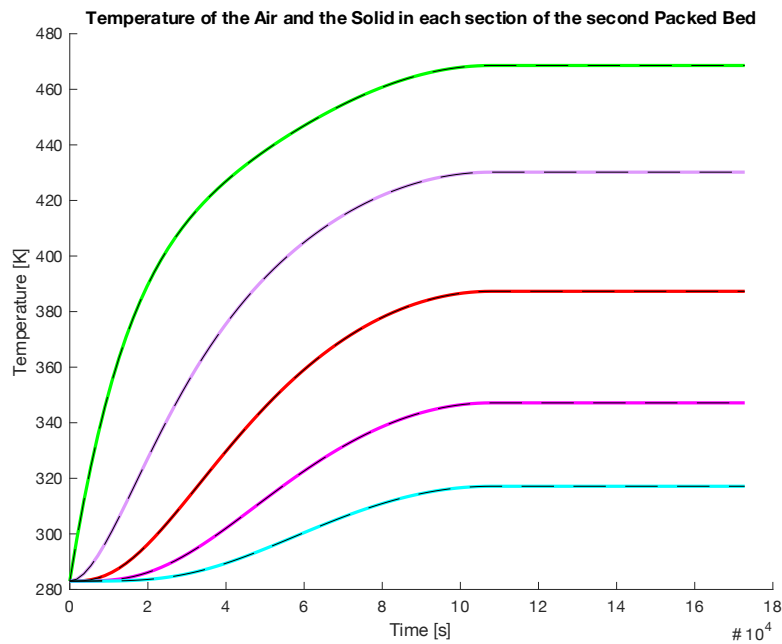
Figure 8.3: The temperature over the second packed bed. The green line is the first section, the purple is the second section, the red line is the third section, the pink is the fourth section and the turquoise line is the last section. The black dotted lines are the temperature of the solid to the corresponding section.

Again, the temperature of the air in the last section of the packed bed, is the temperature of the air entering the next compressor. This will also vary due do the variation of the temperature into the compressor, but it will be in the range of $416 - 463$ K.

The temperatures over the third Packed bed are shown in Figure 8.4. The green line is the temperature of the air in the first section of the packed bed. This reaches a temperature of 430.1 K, which is a lower temperature than the maximum temperature of the air entering the packed bed. The purple one is the temperature of the air in the second section, which reaches a temperature of 396.5 K. The red one is the temperature of the air in the third section. This temperature reaches 360.9 k. The pink one is the temperature of the air in the fourth section, this reaches 329.2 K, and the turquoise one is for the temperature of the last section of the packed bed at 306.6 K. This is the temperature of the air that enters the cavern. The temperatures over this bed is the lowest of the three of them. This is because the pressure ratio is the lowest, so the temperature out the compressor is lower than for the two others. The first section of this packed bed will, as the second one, not reach the maximum temperature of the air entering the packed bed.
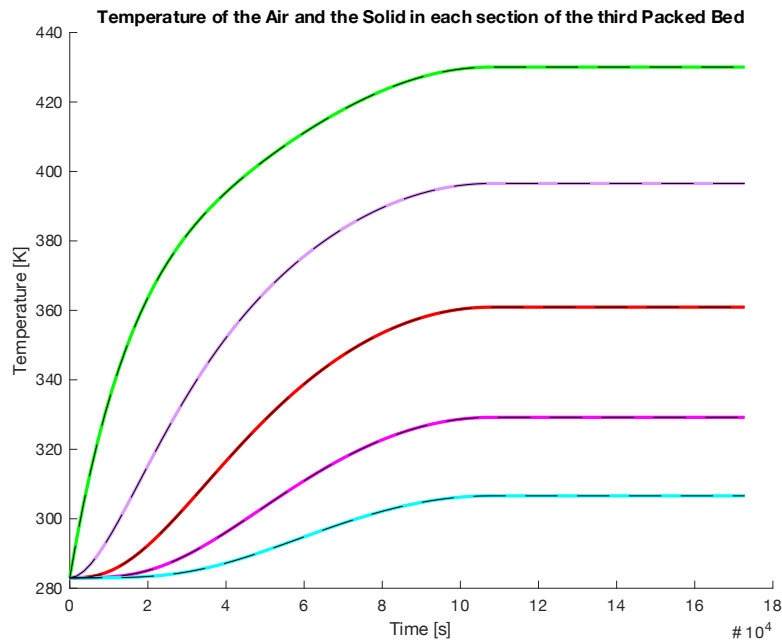
Figure 8.4: The temperature of the air and the solid over the third packed bed. The green line is the first section, the purple is the second section, the red line is the third section, the pink is the fourth section and the blue line is the last section. The black dotted lines are the temperature of the solid to the corresponding section

8.1.3 Work Done by the Compressors

The work done by each of the compressor are shown in Figure 8.5. The turquoise line is the work done by the first compressor, the blue line is the work done by the second compressor, and the pink line is by the last compressor. The polytropic efficiency used for these compressors is 80%.
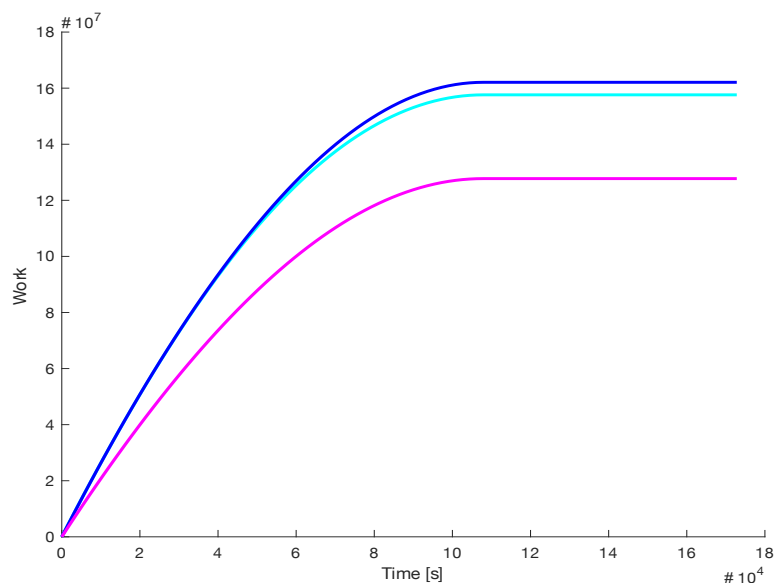
Figure 8.5: The work done by each of the compressors. The turquoise is for the first compressor, the blue line is for the second compressor and the pink is for the third compressor.

To get the total power for the compressors, the values from Figure 8.5 are summed and divided by the time. The total work over time is shown by the purple line in Figure 8.6. From this figure it is found that the power needed to compress the air is 2589 kW or 2.6 MW.
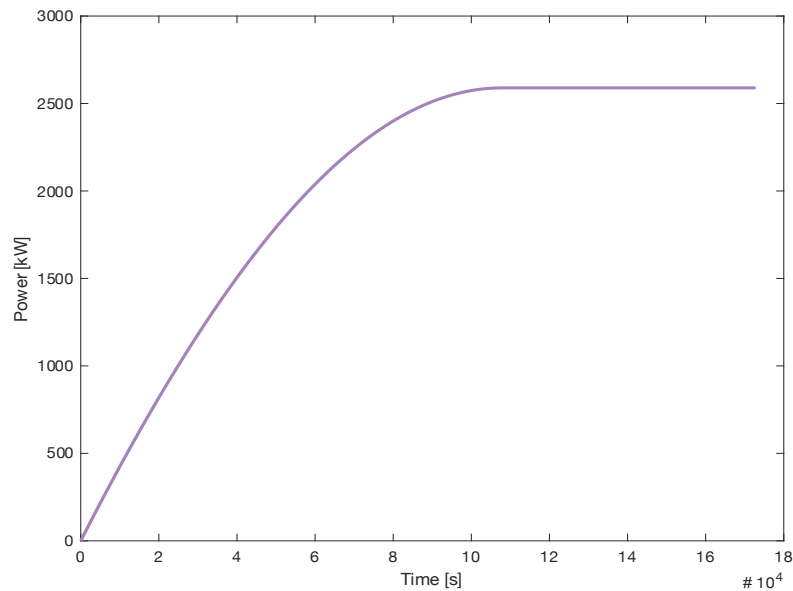
Figure 8.6: The total power needed to compress the air

8.1.4 Temperatures in the Discharge

The initial values for all the sections are the end temperatures calculated in the charge process. The black dotted line is the temperature of the solid in the corresponding section.

In the discharge, the first packed bed is the last one from the charge process. The air from the cavern enters at a temperature of 50°C at the bottom of the packed bed and is heated through the bed. The turquoise line shows the temperature of the air in the bottom of the bed, which is the first section In the discharge process. The pink line is for the temperature of the air in the next section of the bed, the red is the temperature of the air in the middle section of the bed, the purple is for the temperature of the air in the fourth section and the green line is for the temperature of the air in the top section of the packed bed, this will be the temperature of the air entering the first expander. This temperature varies from 430 K, which is the initial temperature of the air and solid in the section, to about 340 K.

Temperature of the Air and the Solid in each section of the third Packed Bed, Disharge
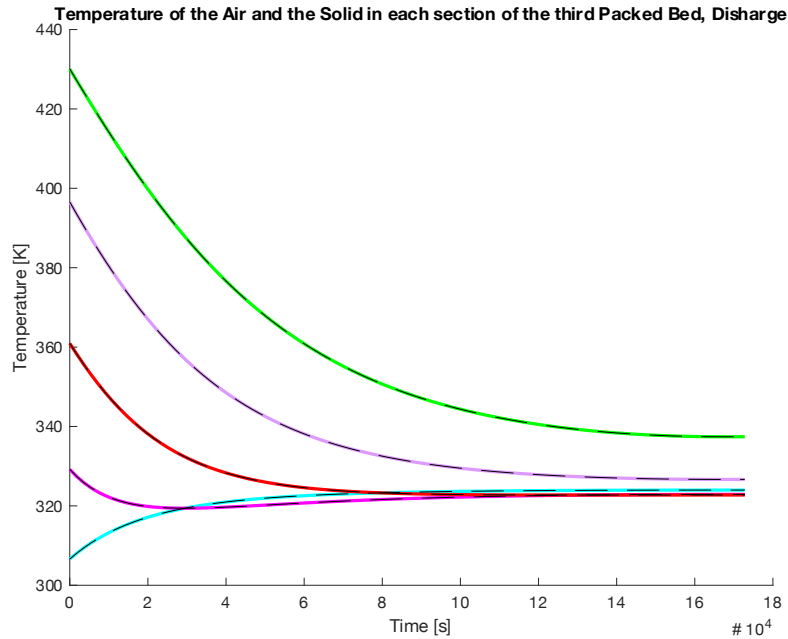
Figure 8.7: Temperatures of the first packed bed in the discharge process (third in the charge process). The turquoise line shows the first section, the pink line is the second, the red is the third, the purple is the fourth, and the green is the last section.

The temperature out the first expander is calculated by eq. (5.38). The temperature into the expander varies and so will the temperature out. The temperature out of the first expander will be between 290 – 230 K. This will be the temperature of the air entering the second packed bed.

Figure 8.8 shows the temperature of the air and the solid over the second packed bed. The turquoise line is the temperature of the air in the first section of the packed bed, it starts at 306 K, which is the end temperature in the charge process. The pink one is the temperature of the air in the second section, the red one is the temperature of the air in the third section, the purple one is the temperature of the air in the fourth section, and the green line is the temperature of the air in the last section of the packed bed. This temperature starts at 468 K, which is the end temperature in the charge process, but will decrease to 340 K. It is this temperature that enters the next expander.
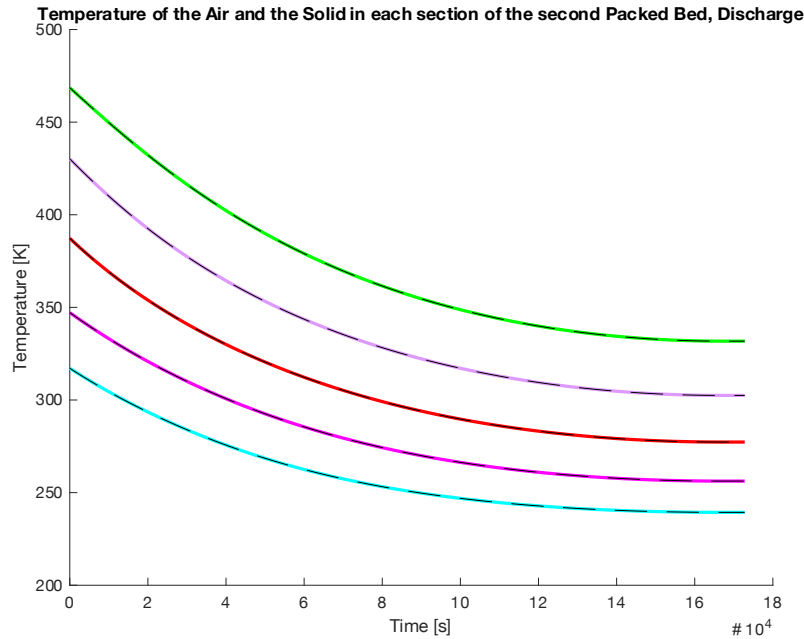
Figure 8.8: Temperatures of the air and the solid over the second packed bed. The turquoise line shows the first section, the pink line is the second, the red is the third, the purple is the fourth, and the green is the last section.

The temperature out of the second expander are also calculated by eq. (5.38), and just as for the first one, this will vary due to the temperature leaving the packed bed. According to the calculations, this temperature will vary from 420 – 295 K.

The temperatures of the air and the solid in the last packed bed in the discharge process are shown in Figure 8.9. The turquoise line shows the temperature of the air in the first section. It starts at 320 K, which is the end temperature of the charge process, and temperature of the air in this section will rise quickly due to the high temperature of the air entering the bed, but as the temperature of the input decreases, so will the temperature of the air and the solid in this section. The pink line is the temperature of the air of the second section, the red one is for the temperature of the air in the third section, the purple line is the temperature of the air in the fourth section and the green one is the temperature of the air in the last section, which starts at 460 K which is the end temperature of the charge process, and the temperature of this section decreases to about 420 K. This is the temperature of the air that enters the last compressor.
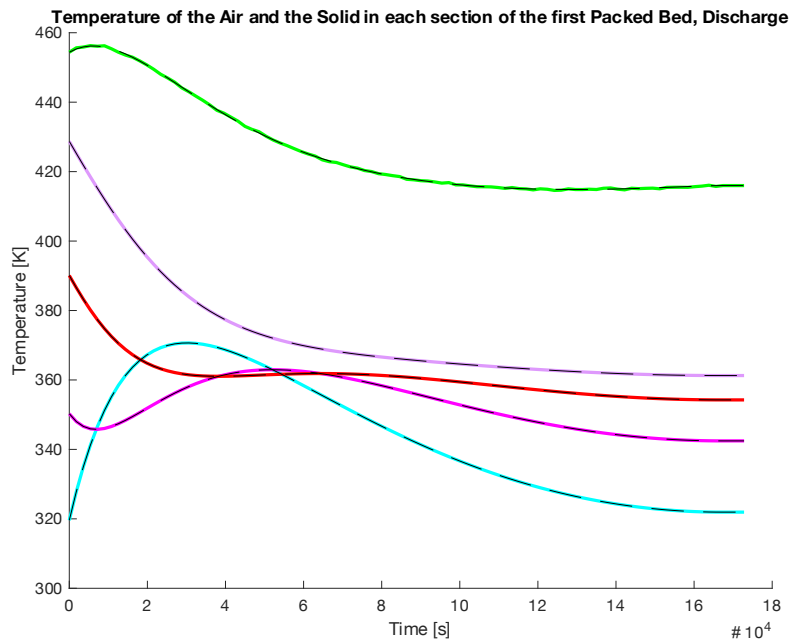
Figure 8.9: The temperature of the air and the solid over the last packed bed in the discharge process. The turquoise line shows the first section, the pink line is the second, the red is the third, the purple is the fourth, and the green is the last section.

8.1.5 Work Produced by the Expanders

The work produced by each of the expanders are shown in Figure 8.10. It is calculated by eq. (5.39), with an isentropic efficiency of 80%. The turquoise line shows the work produced by the first expander. The blue line shows the work produced by the second expander and the pink line is for the last expander. The work is negative because its extracted from the system.
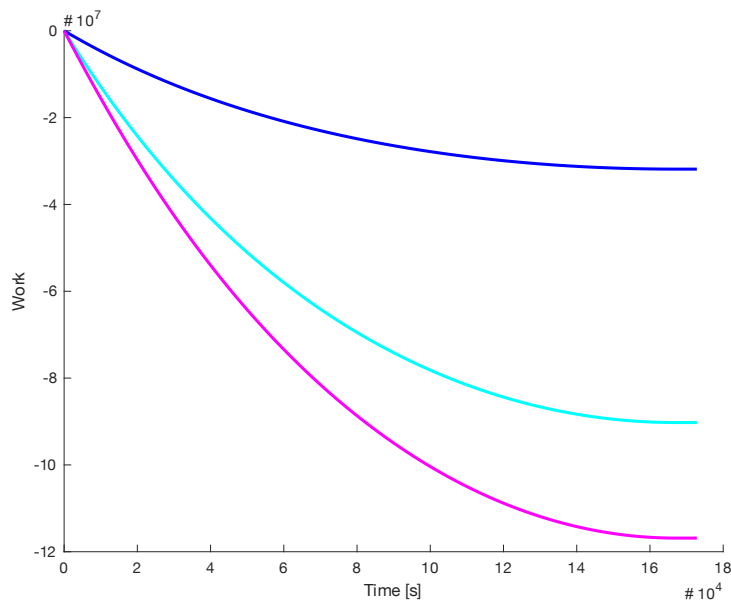
Figure 8.10: The work produced by each compressor. The blue line is for the second expander, the turquoise line is for the first expander, and the pink line is for the third compressor.

To get the total power for the expanders, the values from in Figure 8.10 are summed and divided by the time. The minus is also removed for easier comparisons with the work in the

charge process. The total work over time is shown by the purple line in Figure 8.11. From this figure it is found that the power produced in the expansion of the air is 1383 kW or 1.4 MW.
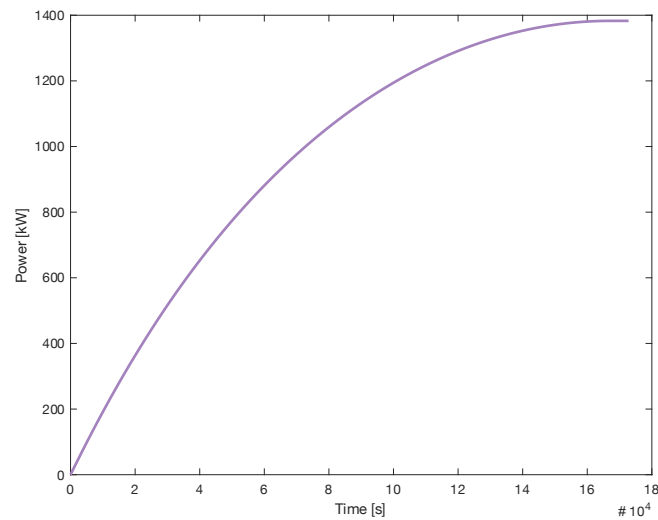
Figure 8.11: The power produced by the expanders over time.

This gives a capacity of 66 389 kWh or 66.4 MWh.

8.2 Efficiency of the System

The efficiency of the system is calculated by eq. (5.40) and based on the results in chapter 8.1.3 and 8.1.5 the efficiency of this system is:

$\eta = 53.4\,\%$

8.3 Cost of the System

Based on the calculation in chapter 5, the cost of the system has been calculated. The cost of the system is shown in Table 8.3. The price mentioned in the third column is for one unit. The cost in the last column is the total cost for the components, e.g. one compressor costs 5 100 000 NOK, and the total cost for three compressors is 15 300 000 NOK. The last row shows the total cost of the system. This is calculated to be 175 176 500 NOK.

Table 8.3: The estimated cost of the system.

Component		Price	Total cost, [NOK]
Compressors	One Compressor	5 100 000 NOK	15 300 000, -
Packed Beds	Mountain blasting	Assuming a price of 200 NOK/m^3	1 413 700, -
	Solid	Assuming a price of 1.9 $/kg	138 910 000, -
Cavern	Mountain blasting	Assuming a price of 200 NOK/m^3	8 252 800, -
Expanders	One expander	5 100 000 NOK	15 300 000, -
Total Cost			179 176 500, -

This cost estimation only includes the main parts of the system: three compressors, three packed beds, three expanders and a cavern. The cost does not include cost for pipes, valves or insulation and is only the capital cost of the system.

With a total capacity of 66 384 kWh, the cost estimate is 2 699 NOK/kWh.

9 Discussion

The model for the charge process works well and provides believable results. The simulations for the packed beds in the charge process looks quite good. The air is cooled down to a temperature acceptable for the next compression. The solid is heated fast and reaches high temperatures.

Most of the time were spent getting the charge process to work well. For the discharge process it was not time to do the same adjustments as for the charge process. With more time, some improvements could be done to get better results. According to the simulation, the output temperature for the first expander is between 290 – 230 K, this is temperatures way too low for the expander to handle. One solution for this could be the stop the discharge process when a certain temperature out of the packed bed is exceeded. Another solution could be a lower pressure ratio over the expander but then the limitations of the expander would not be respected.

The size of the packed beds was the same in the simulation, but it could be interesting to see how the system would react if they were in different sizes fitted to each compressor. Also, the simulation was only done for one type of packing material, ceramic Raschig Rings. The system could be tested with other materials, such as metal Raschig Ring or marbles to find the solution that provides the highest efficiency with the lowest cost.

One of the tasks was to simulate for different scenarios of sizes and storage time. Due to the time limit of the project, this was not done. But it could be interesting to see how this would affect the efficiency of the system and the cost estimation.

In this paper only one cycle (one charge and one discharge) was simulated. It would be interesting to see how the temperatures over the packed would be after more than one cycle, and if the efficiency would be affected.

In this system the physical limitations of the components were taken into account, but the maximum temperature out from the compressor are lower than the minimum temperature into the most expanders. This made it hard to find actual equipment. For this system to work other equipment is needed, either a compressor that can handle temperatures around 500°C, or expanders that operates at temperatures around 200°C. The temperature limitations of the expanders are therefore not reached.

After the literature review, an efficiency between 60 - 70 % was expected. Even though the results were not as expected, they are still good. The existing two plant have an efficiency of 40 – 54 % with additional heating by burning fossil fuel. So, this system has a higher efficiency than Huntorf and about the same as the in MacIntosh, but without the CO_2 emissions. This system is also meant to store the surplus electric energy from wind farms, so this is energy would be wasted if it was not stored.

If there is a possibility to use an existing mine, cavern or tunnel, the total cost of the system could be reduced. There is a lot of abandoned mines and tunnels in Norway so there might be possibilities here, but this has not been researched as a part of this thesis.

The Cost estimate for this system are calculated to be 2 699 NOK/kWh, which was as expected, quite high. There is not a lot of numbers to compare with, but in the A-CAES presented in [50] the cost estimation of the system is 334 000 USD/MWh, which is approx. 3 407 NOK/kWh. This is a much smaller system than the one simulated in this task and in this paper, it has been used steel as packing in the thermal storage and above ground air storage.

10 Conclusion

A literature review was conducted and the most promising technology of CAES were found to be the Adiabatic Compressed Air Energy Storage (A-CAES) with the direct heat exchanger Packed Bed as Thermal Energy Storage (TES), and a cavern of constant volume as storage for the compress air. In this system, surplus electric energy is used to power compressors, the heat generated by the compression is stored in a thermal energy storage, this heat is later used to reheat the air for energy production through expanders, when the energy is needed. The system consists of three compressors, three packed beds, three expanders, and a cavern.

A preliminary thermodynamic analysis, consisting of energy and entropy balances, was made for estimation of the size of a system of 12 MW and a storage time of 48 hours. The size of the cavern was calculated to be 41 264 m^3. This value is calculated for a perfect reversible process, so this size is expected to be bigger in an actual system. Then a dynamic model was created for the system, including the packed beds, the mass and temperature of the cavern, and the work done and produced. The model was simulated in MATLAB. The work done by the compressors was 2 589 kW and the work produced by the expanders was 1 383 kW, which corresponds to a capacity of 66 389 kWh. The efficiency of the system was calculated to be 53.4%.

The total cost on the system was calculated to be 179 176 500 NOK, which corresponds to a cost estimation of 2 699 NOK/kWh. This seems like a quite high number, especially when comparing it to the electricity price in Norway, which usually is around 1 NOK/kWh.

The grid in Norway is three-phase alternating current (AC), with a frequency of 50 Hz. With a frequency regulator the frequency from the generator can vary from 47.5 – 52.0 Hz without any negative outcome. The output of wind turbines is unpredictable, and unstable, but a CAES could reduce the grid curtailment, which would result in less wasted energy, and stabilize the energy output to the grid.

The Adiabatic Compressed Air Energy System seems to be a very promising energy storage technology, and with further analysis and studies, and with compressors and expanders that work on the temperatures in the system, hopefully these kinds of systems will be feasible in the future.

References

[1]   G. Grazzini and A. Milazzo, "Thermodynamic analysis of CAES/TES systems for renewable energy plants," *Renewable Energy,* vol. 33, pp. 1998-2006, 09/01 2008, doi: 10.1016/j.renene.2007.12.003.

[2]   J. Moore and B. Shabani, "A Critical Study of Stationary Energy Storage Polices in Australia in an International Context: The Role of Hydrogen and Battery Technologies," *Energies,* vol. 9, p. 674, 08/24 2016, doi: 10.3390/en9090674.

[3]   J. Ramage, "Hydroelectricity," in *Renewable Energy: Power for a sustainable future*, G. Boyle Ed., 3. ed. Oxford: Oxford University Press/The Open University, 2012.

[4]   A. Ruddell "Investigation on Storage Technologies for Intermittent Renewable Energies: Evaluation and recommended R&D strategy," 2003. [Online]. Available: https://web.archive.org/web/20130114062530/http://www.itpower.co.uk/investire/pdfs/flywheelrep.pdf

[5]   EPRI, "EPRI-DOE Handbook of Energy Storage for Transmission & Distribution Applications," Palo Alto, CA, and the U.S. Department of Energy, Washington DC, 1001834, 2003. [Online]. Available: https://www.sandia.gov/ess-ssl/publications/ESHB%201001834%20reduced%20size.pdf

[6]   D. Wolf and M. Budt, "LTA-CAES – A low-temperature approach to Adiabatic Compressed Air Energy Storage," *Applied Energy,* vol. 125, pp. 158-164, 2014/07/15/ 2014, doi: https://doi.org/10.1016/j.apenergy.2014.03.013.

[7]   Eurobat, "Battery Energy Storage in the EU," 2016. [Online]. Available: https://www.eurobat.org/images/news/publications/eurobat_batteryenergystorage_web.pdf

[8]   Adroit Market Research. "Global Energy Storage Battery Market Size And Forecast, 2015-2025." https://www.adroitmarketresearch.com/industry-reports/energy-storage-battery-market (accessed 30.01, 2020).

[9]   International Hydropower Association. "2019 Hydropower Status Report." https://www.hydropower.org/statusreport (accessed 25.01, 2020).

[10]   International Hydropower Association. "Pumped storage hydropower to turbocharge the clean energy transition." https://www.hydropower.org/news/pumped-storage-hydropower-to-turbocharge-the-clean-energy-transition (accessed 25.01, 2020).

[11]   Directorate-general for Internal Policies, "European Renewable Energy Network," 2012. Accessed: 25.01.2020. [Online]. Available: http://www.europarl.europa.eu/document/activities/cont/201202/20120208ATT37544/20120208ATT37544EN.pdf

[12]   I. Calero, C. A. Cañizares, and K. Bhattacharya, "Compressed Air Energy Storage System Modeling for Power System Studies," *IEEE Transactions on Power Systems,* vol. 34, no. 5, pp. 3359-3371, 2019, doi: 10.1109/TPWRS.2019.2901705.

[13]   X. Luo and J. Wang, "Overview of Current Development on Compressed Air Energy Storage," 2013. [Online]. Available: https://eera-es.eu/wp-

content/uploads/2016/06/Overview-of-Current-Development-on-Compressed-Air-Energy-Storage_EERA-report-20131.pdf

[14] W. He and J. Wang, "Optimal selection of air expansion machine in Compressed Air Energy Storage: A review," *Renewable and Sustainable Energy Reviews,* vol. 87, pp. 77-95, 2018/05/01/ 2018, doi: https://doi.org/10.1016/j.rser.2018.01.013.

[15] *SMARTCAES Compressed Air Energy Storage Solutions*, 2015. [Online]. Available: https://www.all-energy.co.uk/__novadocuments/458993?v=636573965454930000.

[16] J. M. Smith, H. C. Van Ness, M. M. Abbott, and M. T. Swihart, "Volumetric Properties of Pure Fluids," in *Introduction to Chemical Engineering Thermodynamics*, J. M. Smith, H. C. Van Ness, M. M. Abbott, and M. T. Swihart Eds., 8. ed. New York: McGraw-Hill Education, 2018, pp. 81-83.

[17] K. Yang, Y. Zhang, X. Li, and J. Xu, "Theoretical evaluation on the impact of heat exchanger in Advanced Adiabatic Compressed Air Energy Storage system," *Energy Conversion and Management,* vol. 86, pp. 1031-1044, 2014/10/01/ 2014, doi: https://doi.org/10.1016/j.enconman.2014.06.062.

[18] *ADELE - Adiabatic Compressed-Air Energy Storage for Electricity Supply*, 2010. [Online]. Available: http://www.rwe.com/web/cms/mediablob/en/391748/data/235554/1/rwe-power-ag/press/company/Brochure-ADELE.pdf.

[19] J. Degl'Innocenti, "Compressed air energy storage for clean offshore energy supply," M.Sc, Institutt for energi og prosessteknikk, Norges Teknisk-Naturvitenskapelige Universitet, Trondheim, , 2018. [Online]. Available: https://ntnuopen.ntnu.no/ntnu-xmlui/bitstream/handle/11250/2560131/19528_FULLTEXT.pdf?sequence=1&isAllowed=y

[20] E. Barbour, D. Mignard, Y. Ding, and Y. Li, "Adiabatic Compressed Air Energy Storage with packed bed thermal energy storage," *Applied Energy,* vol. 155, pp. 804-815, 2015/10/01/ 2015, doi: https://doi.org/10.1016/j.apenergy.2015.06.019.

[21] A. Sciacovelli *et al.*, "Dynamic simulation of Adiabatic Compressed Air Energy Storage (A-CAES) plant with integrated thermal storage – Link between components performance and plant performance," *Applied Energy,* vol. 185, pp. 16-28, 2017/01/01/ 2017, doi: https://doi.org/10.1016/j.apenergy.2016.10.058.

[22] W.-D. Steinmann, "Thermo-mechanical concepts for bulk energy storage," *Renewable and Sustainable Energy Reviews,* vol. 75, pp. 205-219, 2017/08/01/ 2017, doi: https://doi.org/10.1016/j.rser.2016.10.065.

[23] M. Stewart, "7 - Compressor fundamentals," in *Surface Production Operations*, M. Stewart Ed. Boston: Gulf Professional Publishing, 2019, pp. 457-525.

[24] Energy Storage Association. "Isothermal CAES." https://energystorage.org/why-energy-storage/technologies/isothermal-caes/ (accessed 12.03, 2020).

[25] R. Kushnir, A. Dayan, and A. Ullmann, "Temperature and pressure variations within compressed air energy storage caverns," *International Journal of Heat and Mass Transfer,* vol. 55, pp. 5616–5630, 10/01 2012, doi: 10.1016/j.ijheatmasstransfer.2012.05.055.

[26]   D. Caglayan *et al.*, "Technical Potential of Salt Caverns for Hydrogen Storage in Europe," *International Journal of Hydrogen Energy,* vol. 45, 02/01 2020, doi: 10.1016/j.ijhydene.2019.12.161.

[27]   NVE, "The Norwegian power system. Grid connection and licensing," 2018. [Online]. Available: http://publikasjoner.nve.no/faktaark/2018/faktaark2018_03.pdf

[28]   Energy Facts Norway. "The Electricity Grid." https://energifaktanorge.no/norsk-energiforsyning/kraftnett/ (accessed 10.05, 2020).

[29]   J. Sandstad and Ø. Grøn. "Alternating Current (Vekselstrøm)." https://snl.no/vekselstr%C3%B8m (accessed 10.05, 2020).

[30]   NVE, "Connection of consumers and power grid manufacturers (Tilknytning av forbrukere og produsenter til strømnettet)," 2018. [Online]. Available: http://publikasjoner.nve.no/faktaark/2018/faktaark2018_04.pdf

[31]   Statnett, "Functional requirements in the power system (Funksjonkrav i kraftsystemet)," 2012. [Online]. Available: https://web.archive.org/web/20141211060052/http://www.statnett.no/Global/Dokumenter/Kraftsystemet/Systemansvar/FIKS%202012.pdf

[32]   Level 10 Energy. "How to Manage Curtailment in a Virtual Power Purchase Agreement (VPPA)." https://leveltenenergy.com/blog/ppa-risk-management/renewable-energy-curtailment/ (accessed 10.05, 2020).

[33]   R. N. Brown, *Compressors: Selection and Sizing*. Huston, USA: Gulf Professional Publishing, 1997.

[34]   H. I. H. Saravanamuttoo, G. F. C. Rogers, H. Cohen, P. Straznicky, and A. R. Nix, *Gas turbine theory*, 7. ed. Upper Saddle River: Pearson (in English), 2017.

[35]   M. Stewart, "8 - Dynamic compressors," in *Surface Production Operations*, M. Stewart Ed. Boston: Gulf Professional Publishing, 2019, pp. 527-653.

[36]   M. P. Boyce, "3 - Compressor and Turbine Performance Characteristics," in *Gas Turbine Engineering Handbook (Fourth Edition)*, M. P. Boyce Ed. Oxford: Butterworth-Heinemann, 2012, pp. 139-176.

[37]   N. Kolev, *Packed Bed Columns: For Absorption, Desorption, Rectification and Direct Heat Transfer*, 1. ed. Elsevier Science: Elsevier Science, 2006.

[38]   C. McAniff. "The Basic Difference Between Random And Structured Tower Packing." https://www.kimre.com/the-basic-difference-between-random-and-structured-tower-packing/ (accessed 09.05, 2020).

[39]   A. Stella. "Classic Kit: Raschig's rings." https://www.chemistryworld.com/opinion/classic-kit-raschigs-rings/3004935.article (accessed 09.04, 2020).

[40]   AZO Materials. "Alumina - Aluminium Oxide - Al2O3 - A Refractory Ceramic Oxide." https://www.azom.com/properties.aspx?ArticleID=52 (accessed 04.05, 2020).

[41]   Shenzhen Jincheng Chemical Packing Co. "Ceramic Raschig Rings as Catalyst Support Media for Column Packing." https://tracyjincheng104.en.made-in-china.com/product/OCXxsBwJQPcb/China-Ceramic-Raschig-Rings-as-Catalyst-Support-Media-for-Column-Packing.html (accessed 03.05, 2020).

[42]   A. Giovannelli, L. Tamasi, and C. Salvini, "Performance analysis of industrial steam turbines used as air expander in Compressed Air Energy Storage (CAES) systems," *Energy Reports,* vol. 6, pp. 341-346, 2020/02/01/ 2020, doi: https://doi.org/10.1016/j.egyr.2019.08.066.

[43]   F. Buffa, S. Kemble, G. Manfrida, and A. Milazzo, "Exergy and Exergoeconomic Model of a Ground-Based CAES Plant for Peak-Load Energy Production," *Energies,* vol. 6, pp. 1050-1067, 03/01 2013, doi: 10.3390/en6021050.

[44]   J. P. Coutier and E. A. Farber, "Two applications of a numerical approach of heat transfer process within rock beds," *Solar Energy,* vol. 29, no. 6, pp. 451-462, 1982/01/01/ 1982, doi: https://doi.org/10.1016/0038-092X(82)90053-6.

[45]   MathWorks. "ode45." https://se.mathworks.com/help/matlab/ref/ode45.html (accessed 15.04, 2020).

[46]   E. Syverud, "Cost of Compressor," 11.05, 2020.

[47]   Byggestart. "Graving: Hva koster det? (2020-pris)." https://www.byggstart.no/pris/graving (accessed 04.05, 2020).

[48]   Engineering ToolBox. "Air - Thermophysical Properties." https://www.engineeringtoolbox.com/air-properties-d_156.html (accessed 13.03, 2020).

[49]   Pingxiang Nanxiang Chemical Packing CO. "Ceramic Raschig Ring." http://www.nxpacking.com/ceramic-random-packing/ceramic-raschig-ring.html (accessed 09.04, 2020).

[50]   D. Mignard, "Estimating the capital costs of energy storage technologies for levelling the output of renewable energy sources," *International Journal of Environmental Studies,* vol. 71, 11/01 2014, doi: 10.1080/00207233.2014.967103.

Appendices

Appendix A: Signed task description

Appendix B: Equation for calculating flow through valves

Appendix C: Material cost for different materials

Appendix D: The MATLAB code

Appendix A: Signed task description

**University of
South-Eastern Norway**

Faculty of Technology, Natural Sciences and Maritime Sciences, Campus Porsgrunn

FMH606 Master's Thesis

Title: Modelling and evaluation of Compressed Air Energy Storage (CAES) systems

USN supervisor: Carlos F. Pfeiffer (Porsgrunn) and Elisabet Syverud (Kongsberg)

External partner: -

Task background:
Efficient energy storage systems are mandatory in order to include intermittent renewable energy sources, like solar and wind energy. While the use of electrical batteries is proven and well developed, so far it is not practical to store large amounts of energy to cover seasonal variation in power consumption and production.

Alternative approaches to store excess energy from intermittent sources have been proposed and are currently under research or testing, among others: pumping water to high level reservoirs, which later can be used to produce back electricity using water turbines; using the excess electric energy to produce hydrogen through water electrolysis, and producing electricity back through the use of hydrogen cells; using the excess energy to accelerate large mass rotating cylinders (flywheels), and using the stored kinetic energy to move generators and produce electricity; using the excess energy to compress air in large deposits, and use the pressurized air to move turbo-expanders to generate back electricity when needed.

Task description:
The main goal of this master thesis is to investigate proposed techniques for Compressed Air Energy Storage (CAES) systems, and how they can be integrated to electrical energy distribution grids. The main tasks are:

- Complete a literature review of different approaches for CAES systems
- Select some of the most promising CAES technologies, and develop a dynamic model for simulation
- Simulate the behaviour of the CAES systems with different scenarios (the capacity of the system should be agreed during the thesis work with the supervisors); scenarios should include consideration of storage size and storage time
- Propose strategies to integrate CAES systems to an electric distribution grids, including system response time
- Provide a preliminary economic feasibility analysis for the selected CAES systems
- Complete and deliver the master thesis report
- Prepare and deliver a thesis presentation

Student category: EET

Practical arrangements:

The thesis work will be developed at campus Porsgrunn, with frequent video conferences with the supervisor at campus Kongsberg. The project requires testing the simulation models in Modelica or Matlab/Simulink.

Supervision:

As a general rule, the student is entitled to 15-20 hours of supervision. This includes necessary time for the supervisor to prepare for supervision meetings (reading material to be discussed, etc).

Signatures:

Supervisor (Carlos F. Pfeiffer) $5/2-20$
                                                                Date
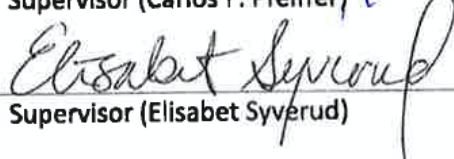
Supervisor (Elisabet Syverud) $3/2-20$
                                                                Date

Student (Marianne F. Heitmann) $3/2-20$
                                                                Date

Appendix B: Equation for calculating flow through valves

Flow Calculation for Gases

The coefficient of flow (Cv) is a formula which is used to determine a valve's flows under various conditions and to select the correct valve for a flow application. The Cv was designed for use with liquid flows, it expresses the flow in gallons per minute of 60º F water with a pressure drop across the valve of 1 psi. However, this same Cv value can be used to determine gas flows through a valve. The formula becomes more intricate for gases, as gases are a compressible fluids and are thus affected by temperature. Furthermore, two formulas are required to accurately estimate flow. When the upstream pressure equals or exceeds two times the downstream pressure, it is known as a "choked flow" situation. This calls for use of the Critical flow formula. If the upstream pressure is less than two times the downstream pressure, the Sub-Critical flow formula should be used.

Critical Flow When: $P_1 \geq 2 \times P_2$	Sub - Critical Flow When: $P_1 < 2 \times P_2$
$$Cv = Q_G \frac{\sqrt{S.G. \times T}}{816 \times P_1}$$	$$Cv = \frac{Q_G}{962} \sqrt{\frac{(S.G. \times T)}{(P_1^2 - P_2^2)}}$$
$$Q_G = Cv \frac{816 \times P_1}{\sqrt{S.G. \times T}}$$	$$Q_G = 962 \times Cv \sqrt{\frac{(P_1^2 - P_2^2)}{(S.G. \times T)}}$$

where:

Q_G = Gas Flow in Standard Cubic Feet per Hour P_1 = Upstream (inlet) pressure in psia
T = Absolute temperature in ºR. (ºF + 460) P_2 = Downstream (outlet) pressure in psia
psia = Absolute pressure. This is psig (gage pressure) plus 14.7 (atmospheric pressure)
S.G. = Specific Gravity of medium where air at 70º F and 14.7 psia = 1.0

Example:

Determine which orifice size should be used for the following application. Upstream pressure is 100 psig, downstream to atmosphere. The medium is 70º F methane gas (S.G.=.554) and the desired flow range is up to 600 SCFH.

$$Cv = 600 \times \frac{\sqrt{.554 \times 530}}{816 \times 114.7} = .1098$$

The Cv value at which 600 SCFH of methane will flow under the above conditions is .1098. Upon examination of our Cv table (on previous page), you can see that this value is reached at approximately turn 9.3 with our -3- (.094) orifice and at turn 5.8 with our -4- (.125) orifice. The end user can choose between approximately 5.8 or 9.3 turns of metering precision for this application.

Specific Gravities of gases	
Gas	**S.G.**
Acetylene	0.907
Air	1.000
Ammonia	0.588
Argon	1.379
Carbon Dioxide	1.529
Carbon Monoxide	0.965
Helium	0.138
Hydrogen	0.070
Hydrogen Chloride	1.268
Methane	0.554
Methyl Chloride	1.736
Nitrogen	0.967
Nitrous Oxide	1.517
Oxygen	1.105
Sulfur Dioxide	2.264

Flow Data, Cv vs. No. of Turns Open
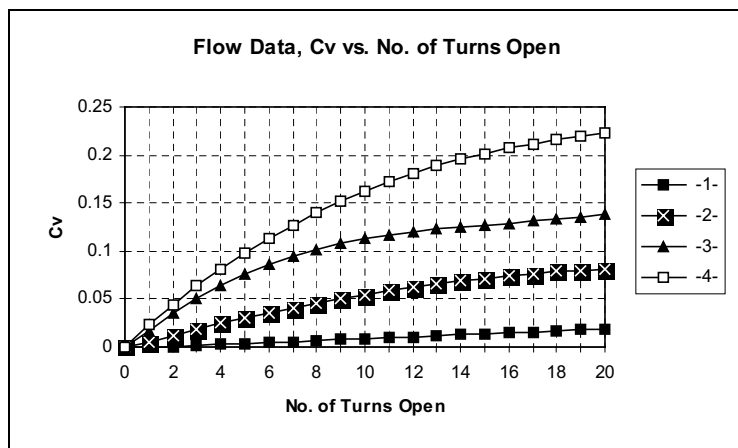
Appendix C: Material cost for different materials

MATERIAL	Type	Cost ($/kg)	Density (ρ, Mg/m^3)	Young's Modulus (E, GPa)	Shear Modulus (G, GPa)	Poisson's Ratio (ν)	Yield Stress (σ_Y, MPa)	UTS (σ_f, MPa)	Breaking strain (ε_f, %)	Fracture Toughness (K_c, MN m$^{-3/2}$)	Thermal Expansion (α, 10^{-6}/C)
Alumina (Al$_2$O$_3$)	ceramic	1.90	3.9	390	125	0.26	4800	35	0.0	4.4	8.1
Aluminum alloy (7075-T6)	metal	1.80	2.7	70	28	0.34	500	570	12	28	33
Beryllium alloy	metal	315.00	2.9	245	110	0.12	360	500	6.0	5.0	14
Bone (compact)	natural	1.90	2.0	14	3.5	0.43	100	100	9.0	5.0	20
Brass (70Cu30Zn, annealed)	metal	2.20	8.4	130	39	0.33	75	325	70.0	80	20
Cermets (Co/WC)	composite	78.60	11.5	470	200	0.30	650	1200	2.5	13	5.8
CFRP Laminate (graphite)	composite	110.00	1.5	1.5	53	0.28	200	550	2.0	38	12
Concrete	ceramic	0.05	2.5	48	20	0.20	25	3.0	0.0	0.75	11
Copper alloys	metal	2.25	8.3	135	50	0.35	510	720	0.3	94	18
Cork	natural	9.95	0.18	0.032	0.005	0.25	1.4	1.5	80	0.074	180
Epoxy thermoset	polymer	5.50	1.2	3.5	1.4	0.25	45	45	4.0	0.50	60
GFRP Laminate (glass)	composite	3.90	1.8	26	10	0.28	125	530	2.0	40	19
Glass (soda)	ceramic	1.35	2.5	65	26	0.23	3500	35	0.0	0.71	8.8
Granite	ceramic	3.15	2.6	66	26	0.25	2500	60	0.1	1.5	6.5
Ice (H$_2$O)	ceramic	0.23	0.92	9.1	3.6	0.28	85	6.5	0.0	0.11	55
Lead alloys	metal	1.20	11.1	16	5.5	0.45	33	42	60	40	29
Nickel alloys	metal	6.10	8.5	180	70	0.31	900	1200	30	93	13
Polyamide (nylon)	polymer	4.30	1.1	3.0	0.76	0.42	40	55	5.0	3.0	103
Polybutadiene elastomer	polymer	1.20	0.91	0.0016	0.0005	0.50	2.1	2.1	500	0.087	140
Polycarbonate	polymer	4.90	1.2	2.7	0.97	0.42	70	77	60	2.6	70
Polyester thermoset	polymer	3.00	1.3	3.5	1.4	0.25	50	0.7	2.0	0.70	150
Polyethylene (HDPE)	polymer	1.00	0.95	0.7	0.31	0.42	25	33	90	3.5	225
Polypropylene	polymer	1.10	0.89	0.9	0.42	0.42	35	45	90	3.0	85
Polyurethane elastomer	polymer	4.00	1.2	0.025	0.0086	0.50	30	30	500	0.30	125
Polyvinyl chloride (rigid PVC)	polymer	1.50	1.4	1.5	0.6	0.42	53	60	50	0.54	75
Silicon	ceramic	2.35	2.3	110	44	0.24	3200	35	0.0	1.5	6
Silicon Carbide (SiC)	ceramic	36.00	2.8	450	190	0.15	9800	35	0.0	4.2	4.2
Spruce (parallel to grain)	natural	1.00	0.60	9	0.8	0.30	48	50	10	2.5	4
Steel, high strength 4340	metal	0.25	7.8	210	76	0.29	1240	1550	2.5	100	14
Steel, mild 1020	metal	0.50	7.8	210	76	0.29	200	380	25	140	14
Steel, stainless austenitic 304	metal	2.70	7.8	210	76	0.28	240	590	60	50	17
Titanium alloy (6Al4V)	metal	16.25	4.5	100	39	0.36	910	950	15	85	9.4
Tungsten Carbide (WC)	ceramic	50.00	15.5	550	270	0.21	6800	35	0.0	3.7	5.8

Appendix D: The MATLAB code

```matlab
% ================ CAES charge ===================

load('input.mat');

% ====== Cavern Fixed Parameters ========== %
p_ini = 4000;          % kPa // Initial Pressure inside the Cavern
T_ini = 10.0 + 273.15; % K   // Initial Temperature inside the Cavern

m_ini = ((p_ini * V_Ca)/(R * T_ini)) * m_w;   % kg // Initial Mass of air in
the Cavern

%
=============================================================================
=

% === Compressor (C) === %
Eta_poly = 0.8;    % -    // Polytopic efficiency
p_C1 = 500;        % kPa  // Pressure after 1 Compressor
p_C2 = 2000;       % kPa  // Pressure After 2 Compressor
p_C3 = 7200;       % kPa

p_loss = 100;      % kPa  // Pressure drop over the Packed Bed

% ====== Packed Bed (PB)  ====== %

TM_0 = [283 283 283 283 283 283 283 283 283 283 283 283 283 283 283 283 283
283 283 283 283 283 283 283 283 283 283 283 283 m_ini T_ini 0 0 0];
tspan = [0:1800:172800];
[t,TM] = ode45(@packed_bed,tspan,TM_0);

%
=============================================================================
=

save('CAES_Charge.mat','t','TM');

T_PB1 = TM(:,5);                          % K // Temperature of the air after 1
Packed Bed
T_PB2 = TM(:,15);                         % K // Temperature of the air after 2
Packed Bed

W_C = (TM(:,33) + TM(:,34) + TM(:,35))/(48*3600);       % kW

T_C1 = T_in  * ( p_C1/p_in )^((R/C_pa));                % K // Temperature
After 1 Compressor
T_C2 = T_PB1 * ( p_C2/(p_C1 - p_loss))^((R/C_pa));    % K // Temperature of
the air after 2 Compressor
T_C3 = T_PB2 * ( p_C3/(p_C2 - p_loss))^((R/C_pa));    % K // Temperature of
the air after 3 Compressor
```

```
% ==================== Packed Bed Charge Process ======================


function [6] = packed_bed(t, TM)

% First Packed Bed
T_a1 = TM(1);        % Temperature of the Air in the 1. section
T_a2 = TM(2);        % Temperature of the Air in the 2. section
T_a3 = TM(3);        % Temperature of the Air in the 3. section
T_a4 = TM(4);        % Temperature of the Air in the 4. section
T_a5 = TM(5);        % Temperature of the Air in the 5. section
T_s1 = TM(6);        % Temperature of the Solid in the 1. section
T_s2 = TM(7);        % Temperature of the Solid in the 2. section
T_s3 = TM(8);        % Temperature of the Solid in the 3. section
T_s4 = TM(9);        % Temperature of the Solid in the 4. section
T_s5 = TM(10);       % Temperature of the Solid in the 5. section

% Second Packed Bed
T_a6  = TM(11);      % Temperature of the Air in the 1. section
T_a7  = TM(12);      % Temperature of the Air in the 2. section
T_a8  = TM(13);      % Temperature of the Air in the 3. section
T_a9  = TM(14);      % Temperature of the Air in the 4. section
T_a10 = TM(15);      % Temperature of the Air in the 5. section
T_s6  = TM(16);      % Temperature of the Solid in the 1. section
T_s7  = TM(17);      % Temperature of the Solid in the 2. section
T_s8  = TM(18);      % Temperature of the Solid in the 3. section
T_s9  = TM(19);      % Temperature of the Solid in the 4. section
T_s10 = TM(20);      % Temperature of the Solid in the 5. section

% Third Packed Bed
T_a11 = TM(21);      % Temperature of the Air in the 1. section
T_a12 = TM(22);      % Temperature of the Air in the 2. section
T_a13 = TM(23);      % Temperature of the Air in the 3. section
T_a14 = TM(24);      % Temperature of the Air in the 4. section
T_a15 = TM(25);      % Temperature of the Air in the 5. section
T_s11 = TM(26);      % Temperature of the Solid in the 1. section
T_s12 = TM(27);      % Temperature of the Solid in the 2. section
T_s13 = TM(28);      % Temperature of the Solid in the 3. section
T_s14 = TM(29);      % Temperature of the Solid in the 4. section
T_s15 = TM(30);      % Temperature of the Solid in the 5. section

M_Ca = TM(31);       % Mass of air inside the cave, kg
T_Ca = TM(32);       % Temperature inside the cave

% ============= Fluid (Air) =========================== %

m_w = 28.9647;       % kg/kmol   //  Molecular Weight Air
R = 8.314;           % kJ/kmol K // Univergal Gas Constant
C_a = 1.006;         % kJ/kg K   // Specific Heat Capacity, constant pressure,
kg.
Cp_a = m_w * C_a;    % kJ/kmol K // Specific Heat Capcity, constant pressure
Cv_a = Cp_a - R;     % kJ/kmol K // Specific Heat Capcity, constant volume

% ==== Compressor ==== %
Eta_poly = 0.8;      % -              // Polytopic efficiency

p_in = 101.325;
p_C1 = 500.0;        % kPa // Pressure in the second compressor, fixed pressure
p_C2 = 2000.0;       % kPa // Pressure in the compressor, fixed pressure
p_C3 = 7200.0;       % kPa // Pressure in the compressor, fixed pressure
```

```matlab
p_PBdrop = 100;                                     % kPa

T_in = 15 + 273.15;                                 % K  // Temperature in the first
compressor
T_C1 = T_in   * (p_C1/p_in )^((R/Cp_a)); % K // Temperature after first
compressor
T_C2 = T_a5   * (p_C2/(p_C1 - p_PBdrop))^((R/Cp_a));  % K  // Temperature
after second compressor
T_C3 = T_a10 * (p_C3/(p_C2 - p_PBdrop))^((R/Cp_a));  % K  // Temperature
after third compressor

PW_C1_mol = Cv_a * (T_C1 - T_in )/Eta_poly;        % kJ/kmol      // Power
of the first compressor
PW_C2_mol = Cv_a * (T_C2 - T_a5 )/Eta_poly;        % kJ/kmol      // Power
of the second compressor
PW_C3_mol = Cv_a * (T_C3 - T_a10)/Eta_poly;        % kJ/kmol      // Power
of the third compressor

% ==== Column ==== %
epsilon = 0.74;    % -          // Void fraction
r = 5;             % m          // Radius of the Packed Bed
Z = 30;            % m          // Height of the Packed bed
A = pi * r^2;      % m          // Sectional area of the Packed Bed
n_PB = 5;          % -          // Number of sections
Dz = Z/n_PB;       % m          // Slice of height

% ==== Solid (Ceramic) ==== %
d_p = 50*10^-3;    % m          // Average particle diameter
C_s = 0.955;       % kJ/kg K    // Heat Capacity of the soild
Rho_s = 3900;      % kg/m^3     // Density of the soild

% ====== Cavern ========= %
R_Ca = 21.4;                       % m            // Radius of the cavern
V_Ca = (4*pi*R_Ca^3)/3.0;          % m^3          // Volume of the cavern

p_Ca = (M_Ca/m_w * R * T_Ca)/V_Ca;

%========== Flow given by the control valve before the cave ===
Cv_valve = 50.73;                  %              // Cv of the control
vcontrol valve

% =======  From paper on flow through a valve
if (7000 - p_Ca) > 0
    air_flow_american =  962.0 * Cv_valve * sqrt(((7000 * 0.14504)^2 - (p_Ca
* 0.14504 )^2)/(T_a5*1.8));        % Standard ft^3/hour
else
    air_flow_american = 0;
end




% ==== Conversion to SI
w_ft = 0.0807;   % lsb/ft^3    // weight of a cubic feet of air at standard
conditions
lb = 0.45359237;  % kg/lsb

air_flow_mass = w_ft * air_flow_american * lb/3600.0;   % kg/s
m_dot = air_flow_mass;                                  % kg/s
```

```matlab
% ========================== Power in kJ/s ========== %
air_flow_molar = air_flow_mass / m_w;

PW_C1 = PW_C1_mol * air_flow_molar;                    % kJ
PW_C2 = PW_C2_mol * air_flow_molar;                    % kJ
PW_C3 = PW_C3_mol * air_flow_molar;                    % kJ

% ====== Heat transfer coeficient ======= %
G = (m_dot)/(A * epsilon);     % kg/m^2s      // Core mass velocity
h_vol = 700 * (G/(d_p))^0.76; % kJ/m^3sK     // Volumetric heat transfer
coefficient

% ====== Pressure drop ====== %
p_drop = 100/n_PB;

p_1 = p_C1 - p_drop;
p_2 = p_C1 - (2 * p_drop);
p_3 = p_C1 - (3 * p_drop);
p_4 = p_C1 - (4 * p_drop);
p_5 = p_C1 - (5 * p_drop);

p_6  = p_C2 - p_drop;
p_7  = p_C2 - (2 * p_drop);
p_8  = p_C2 - (3 * p_drop);
p_9  = p_C2 - (4 * p_drop);
p_10 = p_C2 - (5 * p_drop);

p_11 = p_C3 - p_drop;
p_12 = p_C3 - (2 * p_drop);
p_13 = p_C3 - (3 * p_drop);
p_14 = p_C3 - (4 * p_drop);
p_15 = p_C3 - (5 * p_drop);

% === Density of the fluid (Air) === %
Rho_a1 = p_1 / (R * T_a1) * m_w;
Rho_a2 = p_2 / (R * T_a2) * m_w;
Rho_a3 = p_3 / (R * T_a3) * m_w;
Rho_a4 = p_4 / (R * T_a4) * m_w;
Rho_a5 = p_5 / (R * T_a5) * m_w;

Rho_a6  = p_6 / (R * T_a6) * m_w;
Rho_a7  = p_7 / (R * T_a7) * m_w;
Rho_a8  = p_8 / (R * T_a8) * m_w;
Rho_a9  = p_9 / (R * T_a9) * m_w;
Rho_a10 = p_10 / (R * T_a10) * m_w;

Rho_a11 = p_11 / (R * T_a11) * m_w;
Rho_a12 = p_12 / (R * T_a12) * m_w;
Rho_a13 = p_13 / (R * T_a13) * m_w;
Rho_a14 = p_14 / (R * T_a14) * m_w;
Rho_a15 = p_15 / (R * T_a15) * m_w;

% === Velocity of the fluid (Air) === %
v_a1 = (m_dot / (Rho_a1))/(A * epsilon);
v_a2 = (m_dot / (Rho_a2))/(A * epsilon);
v_a3 = (m_dot / (Rho_a3))/(A * epsilon);
v_a4 = (m_dot / (Rho_a4))/(A * epsilon);
v_a5 = (m_dot / (Rho_a5))/(A * epsilon);

v_a6  = (m_dot / (Rho_a6))/(A * epsilon);
v_a7  = (m_dot / (Rho_a7))/(A * epsilon);
```

```
v_a8  = (m_dot / (Rho_a8))/(A * epsilon);
v_a9  = (m_dot / (Rho_a9))/(A * epsilon);
v_a10 = (m_dot / (Rho_a10))/(A * epsilon);


v_a11 = (m_dot / (Rho_a11))/(A * epsilon);
v_a12 = (m_dot / (Rho_a12))/(A * epsilon);
v_a13 = (m_dot / (Rho_a13))/(A * epsilon);
v_a14 = (m_dot / (Rho_a14))/(A * epsilon);
v_a15 = (m_dot / (Rho_a15))/(A * epsilon);


%========================= DYNAMIC MODEL ====================%
% === Temperature of the fluid (Air) === %
dT_a1 = ((-v_a1 * A * Rho_a1 * C_a * (T_a1 - T_C1)/Dz * Dz) - (h_vol * A *
Dz * (T_a1 - T_s1)))/(epsilon * A * Dz * Rho_a1 * C_a);
dT_a2 = ((-v_a2 * A * Rho_a2 * C_a * (T_a2 - T_a1)/Dz * Dz) - (h_vol * A *
Dz * (T_a2 - T_s2)))/(epsilon * A * Dz * Rho_a2 * C_a);
dT_a3 = ((-v_a3 * A * Rho_a3 * C_a * (T_a3 - T_a2)/Dz * Dz) - (h_vol * A *
Dz * (T_a3 - T_s3)))/(epsilon * A * Dz * Rho_a3 * C_a);
dT_a4 = ((-v_a4 * A * Rho_a4 * C_a * (T_a4 - T_a3)/Dz * Dz) - (h_vol * A *
Dz * (T_a4 - T_s4)))/(epsilon * A * Dz * Rho_a4 * C_a);
dT_a5 = ((-v_a5 * A * Rho_a5 * C_a * (T_a5 - T_a4)/Dz * Dz) - (h_vol * A *
Dz * (T_a5 - T_s5)))/(epsilon * A * Dz * Rho_a5 * C_a);


dT_a6  = ((-v_a6  * A * Rho_a6  * C_a * (T_a6  - T_C2)/Dz * Dz) - (h_vol *
A * Dz * (T_a6  - T_s6 )))/(epsilon * A * Dz * Rho_a6  * C_a);
dT_a7  = ((-v_a7  * A * Rho_a7  * C_a * (T_a7  - T_a6)/Dz * Dz) - (h_vol *
A * Dz * (T_a7  - T_s7 )))/(epsilon * A * Dz * Rho_a7  * C_a);
dT_a8  = ((-v_a8  * A * Rho_a8  * C_a * (T_a8  - T_a7)/Dz * Dz) - (h_vol *
A * Dz * (T_a8  - T_s8 )))/(epsilon * A * Dz * Rho_a8  * C_a);
dT_a9  = ((-v_a9  * A * Rho_a9  * C_a * (T_a9  - T_a8)/Dz * Dz) - (h_vol *
A * Dz * (T_a9  - T_s9 )))/(epsilon * A * Dz * Rho_a9  * C_a);
dT_a10 = ((-v_a10 * A * Rho_a10 * C_a * (T_a10 - T_a9)/Dz * Dz) - (h_vol *
A * Dz * (T_a10 - T_s10)))/(epsilon * A * Dz * Rho_a10 * C_a);


dT_a11 = ((-v_a11 * A * Rho_a11 * C_a * (T_a11 - T_C3 )/Dz * Dz) - (h_vol *
A * Dz * (T_a11 - T_s11)))/(epsilon * A * Dz * Rho_a11 * C_a);
dT_a12 = ((-v_a12 * A * Rho_a12 * C_a * (T_a12 - T_a11)/Dz * Dz) - (h_vol *
A * Dz * (T_a12 - T_s12)))/(epsilon * A * Dz * Rho_a12 * C_a);
dT_a13 = ((-v_a13 * A * Rho_a13 * C_a * (T_a13 - T_a12)/Dz * Dz) - (h_vol *
A * Dz * (T_a13 - T_s13)))/(epsilon * A * Dz * Rho_a13 * C_a);
dT_a14 = ((-v_a14 * A * Rho_a14 * C_a * (T_a14 - T_a13)/Dz * Dz) - (h_vol *
A * Dz * (T_a14 - T_s14)))/(epsilon * A * Dz * Rho_a14 * C_a);
dT_a15 = ((-v_a15 * A * Rho_a15 * C_a * (T_a15 - T_a14)/Dz * Dz) - (h_vol *
A * Dz * (T_a15 - T_s15)))/(epsilon * A * Dz * Rho_a15 * C_a);


% === Temperature of the soild (Ceramic) === %
dT_s1 = (-h_vol * (T_s1 - T_a1))/((1 - epsilon) * Rho_s * C_s);
dT_s2 = (-h_vol * (T_s2 - T_a2))/((1 - epsilon) * Rho_s * C_s);
dT_s3 = (-h_vol * (T_s3 - T_a3))/((1 - epsilon) * Rho_s * C_s);
dT_s4 = (-h_vol * (T_s4 - T_a4))/((1 - epsilon) * Rho_s * C_s);
dT_s5 = (-h_vol * (T_s5 - T_a5))/((1 - epsilon) * Rho_s * C_s);


dT_s6  = (-h_vol * (T_s6  - T_a6 ))/((1 - epsilon) * Rho_s * C_s);
dT_s7  = (-h_vol * (T_s7  - T_a7 ))/((1 - epsilon) * Rho_s * C_s);
dT_s8  = (-h_vol * (T_s8  - T_a8 ))/((1 - epsilon) * Rho_s * C_s);
dT_s9  = (-h_vol * (T_s9  - T_a9 ))/((1 - epsilon) * Rho_s * C_s);
dT_s10 = (-h_vol * (T_s10 - T_a10))/((1 - epsilon) * Rho_s * C_s);


dT_s11 = (-h_vol * (T_s11 - T_a11))/((1 - epsilon) * Rho_s * C_s);
dT_s12 = (-h_vol * (T_s12 - T_a12))/((1 - epsilon) * Rho_s * C_s);
dT_s13 = (-h_vol * (T_s13 - T_a13))/((1 - epsilon) * Rho_s * C_s);
```

```matlab
dT_s14 = (-h_vol * (T_s14 - T_a14))/((1 - epsilon) * Rho_s * C_s);
dT_s15 = (-h_vol * (T_s15 - T_a15))/((1 - epsilon) * Rho_s * C_s);

% ========================= Mass and energy balance off the cave ==%
dM_Ca = m_dot;
dT_Ca = m_dot/m_w * (Cp_a * T_a15 - Cv_a * T_Ca)/(M_Ca/m_w * Cv_a);

% ========================= Power ========== %

dW_C1 = PW_C1;
dW_C2 = PW_C2;
dW_C3 = PW_C3;

dT = [dT_a1, dT_a2, dT_a3, dT_a4, dT_a5, dT_s1, dT_s2, dT_s3, dT_s4, dT_s5,
dT_a6, dT_a7, dT_a8, dT_a9, dT_a10, dT_s6, dT_s7, dT_s8, dT_s9,
dT_s10,dT_a11, dT_a12, dT_a13, dT_a14, dT_a15, dT_s11, dT_s12, dT_s13,
dT_s14, dT_s15, dM_Ca, dT_Ca, dW_C1, dW_C2, dW_C3]';

end
```

```matlab
% ============== CAES Discharge =========================================


load('CAES_Charge.mat');

% ==== Packed Bed Expander ==== %

TMD_0 = [TM(end,25) TM(end,24) TM(end,23) TM(end,22) TM(end,21) TM(end,30)
TM(end,29)  TM(end,28)  TM(end,27)  TM(end,26)    TM(end,15)  TM(end,14)
TM(end,13) TM(end,12) TM(end,11) TM(end,20) TM(end,19) TM(end,18) TM(end,17)
TM(end,16)  TM(end,5)  TM(end,4)  TM(end,3)  TM(end,2)  TM(end,1)  TM(end,10)
TM(end,9) TM(end,8) TM(end,7) TM(end,6) TM(end,31:32) 0 0 0];
tspan = [0:1800:172800];
[t2,TMD] = ode45(@packed_bed_discharge,tspan,TMD_0);


% ======================================================================

% === Expander (E) === %
p_V  = 4100;    % kPa  // Pressure Valve, in first Expander
p_E1 = 1000;    % kPa  // Pressure out of the first Expander
p_E2 = 600;     % kPa  // Pressure out of the second Expander
p_E3 = p_in;    % kPa  // Pressure out of the third Expander

p_loss = 100;   % kPa  // Pressure drop over packed bed

Eta_isen = 0.80;    % -  // Isentropic Eficiency

T_E1 = TMD(:,5)  * (p_E1/(p_V  - p_loss))^((R/C_pa)); % K   // Temperature
out of the first Expander
T_E2 = TMD(:,15) * (p_E2/(p_E1 - p_loss))^((R/C_pa)); % K   // Temperature
out of the second Expander
T_E3 = TMD(:,25) * (p_E3/(p_E2 - p_loss))^((R/C_pa)); % K   // Temperature
out of the third Expander
```

```matlab
% ============== Packed          Bed          Discharge
=======================================

function [6] = packed_bed_discharge(t2, TMD)



T_a_d15 = TMD(1);   % Temperature of the Air in the 5. section
T_a_d14 = TMD(2);   % Temperature of the Air in the 4. section
T_a_d13 = TMD(3);   % Temperature of the Air in the 3. section
T_a_d12 = TMD(4);   % Temperature of the Air in the 2. section
T_a_d11 = TMD(5);   % Temperature of the Air in the 1. section
T_s_d15 = TMD(6);   % Temperature of the Solid in the 5. section
T_s_d14 = TMD(7);   % Temperature of the Solid in the 4. section
T_s_d13 = TMD(8);   % Temperature of the Solid in the 3. section
T_s_d12 = TMD(9);   % Temperature of the Solid in the 2. section
T_s_d11 = TMD(10);  % Temperature of the Solid in the 1. section


T_a_d10 = TMD(11);  % Temperature of the Air in the 5. section
T_a_d9  = TMD(12);  % Temperature of the Air in the 4. section
T_a_d8  = TMD(13);  % Temperature of the Air in the 3. section
T_a_d7  = TMD(14);  % Temperature of the Air in the 2. section
T_a_d6  = TMD(15);  % Temperature of the Air in the 1. section
T_s_d10 = TMD(16);  % Temperature of the Solid in the 5. section
T_s_d9  = TMD(17);  % Temperature of the Solid in the 4. section
T_s_d8  = TMD(18);  % Temperature of the Solid in the 3. section
T_s_d7  = TMD(19);  % Temperature of the Solid in the 2. section
T_s_d6  = TMD(20);  % Temperature of the Solid in the 1. section


T_a_d5 = TMD(21);   % Temperature of the Air in the 5. section
T_a_d4 = TMD(22);   % Temperature of the Air in the 4. section
T_a_d3 = TMD(23);   % Temperature of the Air in the 3. section
T_a_d2 = TMD(24);   % Temperature of the Air in the 2. section
T_a_d1 = TMD(25);   % Temperature of the Air in the 1. section
T_s_d5 = TMD(26);   % Temperature of the Solid in the 5. section
T_s_d4 = TMD(27);   % Temperature of the Solid in the 4. section
T_s_d3 = TMD(28);   % Temperature of the Solid in the 3. section
T_s_d2 = TMD(29);   % Temperature of the Solid in the 2. section
T_s_d1 = TMD(30);   % Temperature of the Solid in the 1. section


M_Ca  = TMD(31);    % Mass of air inside the cave, kg
T_Ca  = TMD(32);    % Temperature inside the cave

% ================= Fluid (Air)  ================= %
m_w = 28.9647;      % kg/kmol    //  Molecular Weight Air
R = 8.314;          % kJ/kmol K  // Univergal Gas Constant
C_a = 1.006;        % kJ/kg K    // Specific Heat Capacity, constant pressure,
Cp_a = m_w * C_a;   % kJ/kmol K  // Specific Heat Capcity, constant pressure
Cv_a = Cp_a - R;    % kJ/kmol K  // Specific Heat Capcity, constant volume


% ================= Expander E ================= %
Eta_isen = 0.80;    % -              // Isentropic efficiency

p_V  = 4100.0;      % kPa  // Pressure in the expander, fixed
p_E1 = 1000.0;      % kPa  // Pressure out of the first expander, fixed
p_E2 = 600.0;       % kPa  // Pressure out of the second expander, fixed
p_E3 = 101.325;     % kPa  // Pressure out of the third expander, fixed


p_PBdrop = 100;     % Pressure drop over the first Packed Bed


T_Ein = T_a_d11;
```

```matlab
T_E1 = T_Ein   * (p_E1/(p_V  - p_PBdrop))^(R/Cp_a);   % K   // Temperature
after first compressor
T_E2 = T_a_d6  * (p_E2/(p_E1 - p_PBdrop))^(R/Cp_a);   % K   // Temperature
after second compressor
T_E3 = T_a_d1  * (p_E3/(p_E2 - p_PBdrop))^(R/Cp_a);   % K   // Temperature
after third compressor

PW_E1_mol = Cv_a * (T_E1 - T_a_d11)*(Eta_isen);      % kJ/kmol // Power of
the first compressor
PW_E2_mol = Cv_a * (T_E2 - T_a_d6 )*(Eta_isen);      % kJ/kmol // Power of
the second compressor
PW_E3_mol = Cv_a * (T_E3 - T_a_d1 )*(Eta_isen);      % kJ/kmol // Power of
the third compressor


% ================== Column ================== %
epsilon = 0.74;    % -              // Void fraction
r = 5;             % m              // Radius of the Packed Bed
Z = 30;            % m              // Height of the Packed bed
A = pi * r^2;      % m              // Sectional area of the Packed Bed
n_PB = 5;          % -              // Number of sections
Dz = Z/n_PB;       % m              // Slice of height


% ================== Solid (Ceramic) ================== %
d_p = 50*10^-3;    % m              // Average particle diameter
C_s = 0.955;       % kJ/kg K        // Heat Capacity of the soild
Rho_s = 3900;      % kg/m^3         // Density of the soild


% ==================== Cavern ======================== %
R_Ca = 21.4;                       % m              // Radius of the cavern
V_Ca = (4*pi*R_Ca^3)/3.0;          % m^3            // Volume of the cavern
p_Ca = (M_Ca/m_w * R * T_Ca)/V_Ca; % kPa           // Pressure of the cavern

%========== Flow given by the control valve before the cave ===
Cv_valve = 50.73;          % // Cv of the control control valve


% =======  From paper on flow through a valve
if (p_Ca - p_V) > 0
    air_flow_american =  962.0 * Cv_valve * sqrt(((p_Ca * 0.14504)^2 - (p_V
* 0.14504 )^2)/(T_Ca * 1.8));       % Standard ft^3/hour
else
    air_flow_american = 0;
end


% ================== Conversion to SI ==============
w_ft = 0.0807;          % lsb/ft^3      // weight of a cubic feet of air at
standard conditions
lb = 0.45359237;        % kg/lsb


air_flow_mass = w_ft * air_flow_american * lb/3600.0;   % kg/s
m_dot = air_flow_mass;                                  % kg/s

% ======================== Power in kJ/s ========== %
air_flow_molar = air_flow_mass / m_w;


PW_E1 = PW_E1_mol * air_flow_molar;                     % kJ/s
PW_E2 = PW_E2_mol * air_flow_molar;                     % kJ/s
PW_E3 = PW_E3_mol * air_flow_molar;                     % kJ/s


% ====== Heat transfer coeficient ======= %
G = (m_dot)/(A * epsilon);        % kg/m^2s      // Core mass velocity
```

```matlab
h_vol = 700 * (G/(d_p))^0.76;      % kJ/m^3sK    // Volumetric heat transfer
coefficient

% ====== Pressure drop ====== %
p_drop  = 100/n_PB;


p_1 = p_E2 - (5 * p_drop);
p_2 = p_E2 - (4 * p_drop);
p_3 = p_E2 - (3 * p_drop);
p_4 = p_E2 - (2 * p_drop);
p_5 = p_E2 - (p_drop);


p_6  = p_E1 - (5 * p_drop);
p_7  = p_E1 - (4 * p_drop);
p_8  = p_E1 - (3 * p_drop);
p_9  = p_E1 - (2 * p_drop);
p_10 = p_E1 - (p_drop);


p_11 = p_V - (5 * p_drop);
p_12 = p_V - (4 * p_drop);
p_13 = p_V - (3 * p_drop);
p_14 = p_V - (2 * p_drop);
p_15 = p_V - (p_drop);

% === Density of the fluid (Air) === %
Rho_a1 = p_1 / (R * T_a_d1) * m_w;
Rho_a2 = p_2 / (R * T_a_d2) * m_w;
Rho_a3 = p_3 / (R * T_a_d3) * m_w;
Rho_a4 = p_4 / (R * T_a_d4) * m_w;
Rho_a5 = p_5 / (R * T_a_d5) * m_w;


Rho_a6  = p_6  / (R * T_a_d6) * m_w;
Rho_a7  = p_7  / (R * T_a_d7) * m_w;
Rho_a8  = p_8  / (R * T_a_d8) * m_w;
Rho_a9  = p_9  / (R * T_a_d9) * m_w;
Rho_a10 = p_10 / (R * T_a_d10) * m_w;


Rho_a11 = p_11 / (R * T_a_d11) * m_w;
Rho_a12 = p_12 / (R * T_a_d12) * m_w;
Rho_a13 = p_13 / (R * T_a_d13) * m_w;
Rho_a14 = p_14 / (R * T_a_d14) * m_w;
Rho_a15 = p_15 / (R * T_a_d15) * m_w;

% === Velocity of the fluid (Air) === %
v_a1 = (m_dot / (Rho_a1))/(A * epsilon);
v_a2 = (m_dot / (Rho_a2))/(A * epsilon);
v_a3 = (m_dot / (Rho_a3))/(A * epsilon);
v_a4 = (m_dot / (Rho_a4))/(A * epsilon);
v_a5 = (m_dot / (Rho_a5))/(A * epsilon);


v_a6  = (m_dot / (Rho_a6))/(A * epsilon);
v_a7  = (m_dot / (Rho_a7))/(A * epsilon);
v_a8  = (m_dot / (Rho_a8))/(A * epsilon);
v_a9  = (m_dot / (Rho_a9))/(A * epsilon);
v_a10 = (m_dot / (Rho_a10))/(A * epsilon);


v_a11 = (m_dot / (Rho_a11))/(A * epsilon);
v_a12 = (m_dot / (Rho_a12))/(A * epsilon);
v_a13 = (m_dot / (Rho_a13))/(A * epsilon);
v_a14 = (m_dot / (Rho_a14))/(A * epsilon);
v_a15 = (m_dot / (Rho_a15))/(A * epsilon);
```

```
%========================= DYNAMIC MODEL =====================%

% === Temperature of the fluid (Air) === %

dT_a_d15 = ((-v_a15 * A * Rho_a15 * C_a * (- T_Ca    + T_a_d15)/Dz * Dz) -
(h_vol * A * Dz * (T_a_d15 - T_s_d15)))/(epsilon * A * Dz * Rho_a15 * C_a);
dT_a_d14 = ((-v_a14 * A * Rho_a14 * C_a * (- T_a_d15 + T_a_d14)/Dz * Dz) -
(h_vol * A * Dz * (T_a_d14 - T_s_d14)))/(epsilon * A * Dz * Rho_a14 * C_a);
dT_a_d13 = ((-v_a13 * A * Rho_a13 * C_a * (- T_a_d14 + T_a_d13)/Dz * Dz) -
(h_vol * A * Dz * (T_a_d13 - T_s_d13)))/(epsilon * A * Dz * Rho_a13 * C_a);
dT_a_d12 = ((-v_a12 * A * Rho_a12 * C_a * (- T_a_d13 + T_a_d12)/Dz * Dz) -
(h_vol * A * Dz * (T_a_d12 - T_s_d12)))/(epsilon * A * Dz * Rho_a12 * C_a);
dT_a_d11 = ((-v_a11 * A * Rho_a11 * C_a * (- T_a_d12 + T_a_d11)/Dz * Dz) -
(h_vol * A * Dz * (T_a_d11 - T_s_d11)))/(epsilon * A * Dz * Rho_a11 * C_a);

dT_a_d10 = ((-v_a10 * A * Rho_a10 * C_a * (- T_E1    + T_a_d10)/Dz * Dz) -
(h_vol * A * Dz * (T_a_d10 - T_s_d10)))/(epsilon * A * Dz * Rho_a10 * C_a);
dT_a_d9  = ((-v_a9  * A * Rho_a9  * C_a * (- T_a_d10 + T_a_d9 )/Dz * Dz) -
(h_vol * A * Dz * (T_a_d9  - T_s_d9 )))/(epsilon * A * Dz * Rho_a9  * C_a);
dT_a_d8  = ((-v_a8  * A * Rho_a8  * C_a * (- T_a_d9  + T_a_d8 )/Dz * Dz) -
(h_vol * A * Dz * (T_a_d8  - T_s_d8 )))/(epsilon * A * Dz * Rho_a8  * C_a);
dT_a_d7  = ((-v_a7  * A * Rho_a7  * C_a * (- T_a_d8  + T_a_d7 )/Dz * Dz) -
(h_vol * A * Dz * (T_a_d7  - T_s_d7 )))/(epsilon * A * Dz * Rho_a7  * C_a);
dT_a_d6  = ((-v_a6  * A * Rho_a6  * C_a * (- T_a_d7  + T_a_d6 )/Dz * Dz) -
(h_vol * A * Dz * (T_a_d6  - T_s_d6 )))/(epsilon * A * Dz * Rho_a6  * C_a);

dT_a_d5  = ((-v_a5  * A * Rho_a5  * C_a * (- T_E2    + T_a_d5 )/Dz * Dz) -
(h_vol * A * Dz * (T_a_d5  - T_s_d5 )))/(epsilon * A * Dz * Rho_a5  * C_a);
dT_a_d4  = ((-v_a4  * A * Rho_a4  * C_a * (- T_a_d5  + T_a_d4 )/Dz * Dz) -
(h_vol * A * Dz * (T_a_d4  - T_s_d4 )))/(epsilon * A * Dz * Rho_a4  * C_a);
dT_a_d3  = ((-v_a3  * A * Rho_a3  * C_a * (- T_a_d4  + T_a_d3 )/Dz * Dz) -
(h_vol * A * Dz * (T_a_d3  - T_s_d3 )))/(epsilon * A * Dz * Rho_a3  * C_a);
dT_a_d2  = ((-v_a2  * A * Rho_a2  * C_a * (- T_a_d3  + T_a_d2 )/Dz * Dz) -
(h_vol * A * Dz * (T_a_d2  - T_s_d2 )))/(epsilon * A * Dz * Rho_a2  * C_a);
dT_a_d1  = ((-v_a1  * A * Rho_a1  * C_a * (- T_a_d2  + T_a_d1 )/Dz * Dz) -
(h_vol * A * Dz * (T_a_d1  - T_s_d1 )))/(epsilon * A * Dz * Rho_a1  * C_a);


% === Temperature of the soild (Ceramic) === %

dT_s_d15 = (-h_vol * (T_s_d15 - T_a_d15))/((1 - epsilon) * Rho_s * C_s);
dT_s_d14 = (-h_vol * (T_s_d14 - T_a_d14))/((1 - epsilon) * Rho_s * C_s);
dT_s_d13 = (-h_vol * (T_s_d13 - T_a_d13))/((1 - epsilon) * Rho_s * C_s);
dT_s_d12 = (-h_vol * (T_s_d12 - T_a_d12))/((1 - epsilon) * Rho_s * C_s);
dT_s_d11 = (-h_vol * (T_s_d11 - T_a_d11))/((1 - epsilon) * Rho_s * C_s);

dT_s_d10 = (-h_vol * (T_s_d10 - T_a_d10))/((1 - epsilon) * Rho_s * C_s);
dT_s_d9  = (-h_vol * (T_s_d9  - T_a_d9 ))/((1 - epsilon) * Rho_s * C_s);
dT_s_d8  = (-h_vol * (T_s_d8  - T_a_d8 ))/((1 - epsilon) * Rho_s * C_s);
dT_s_d7  = (-h_vol * (T_s_d7  - T_a_d7 ))/((1 - epsilon) * Rho_s * C_s);
dT_s_d6  = (-h_vol * (T_s_d6  - T_a_d6 ))/((1 - epsilon) * Rho_s * C_s);

dT_s_d5  = (-h_vol * (T_s_d5 - T_a_d5))/((1 - epsilon) * Rho_s * C_s);
dT_s_d4  = (-h_vol * (T_s_d4 - T_a_d4))/((1 - epsilon) * Rho_s * C_s);
dT_s_d3  = (-h_vol * (T_s_d3 - T_a_d3))/((1 - epsilon) * Rho_s * C_s);
dT_s_d2  = (-h_vol * (T_s_d2 - T_a_d2))/((1 - epsilon) * Rho_s * C_s);
dT_s_d1  = (-h_vol * (T_s_d1 - T_a_d1))/((1 - epsilon) * Rho_s * C_s);

% ========================== Mass and energy balance off the cave ==%
dM_Ca = - m_dot;
```

```matlab
% dT_Ca = (m_dot/m_w) * ((Cp_a – Cv_a)* T_Ca)/((M_Ca/m_w) * Cv_a);
dT_Ca = 0;
% ========================= Power ========== %
dW_E1 = PW_E1;
dW_E2 = PW_E2;
dW_E3 = PW_E3;


dT = [dT_a_d15, dT_a_d14, dT_a_d13, dT_a_d12, dT_a_d11, dT_s_d15, dT_s_d14,
dT_s_d13, dT_s_d12, dT_s_d11, dT_a_d10, dT_a_d9, dT_a_d8, dT_a_d7, dT_a_d6,
dT_s_d10, dT_s_d9, dT_s_d8, dT_s_d7, dT_s_d6, dT_a_d5, dT_a_d4, dT_a_d3,
dT_a_d2, dT_a_d1, dT_s_d5, dT_s_d4, dT_s_d3, dT_s_d2, dT_s_d1, dM_Ca, dT_Ca,
dW_E1, dW_E2, dW_E3]';

end
```